WILEY

IET-Wiley Virtual Symposium on Renewable Energy 2022

Digital and flexible control and operation of transmission and distribution grids for renewable power systems.

September 13 2022

Research conducted at institutions in Germany has led to exciting advances in the areas of renewable energy. This free virtual symposium supported by two of the IET's flagship open access journals *IET Renewable Power Generation (RPG)* and *IET Generation, Transmission & Distribution (GTD)* will be free to attend. It will provide a forum for researchers based in Germany to highlight their research and will celebrate the capacity for renewable energy research to engineer a better world.

Session Topics Include:

- Power Flow Control for efficient Transmission Grids
- Digitalization of Power Systems
- Flexibility in Power Systems
- Smart Distribution Grids

Register free today

The Institution of Engineering and Technology

Received: 25 February 2022 | Revised: 5 May 2022 | Accepted: 4 June 2022

DOI: 10.1049/rpg2.12525

IET Renewable Power Generation

The Institution of Engineering and Technology WILEY

ORIGINAL RESEARCH

Optimal communication-aided protection of meshed smart grids considering stability constraints of distributed generations incorporating optimal selection of relay characteristics

Hamidreza Aghaei[1] | **Hamed Hashemi-Dezaki**[1,2]

[1]Department of Electrical and Computer Engineering, University of Kashan, Kashan, Iran

[2]Research and Innovation Center for Electrical Engineering (RICE), Faculty of Electrical Engineering, University of West Bohemia (UWB), Pilsen, Czech Republic

Correspondence
Hamed Hashemi-Dezaki, Department of Electrical and Computer Engineering, University of Kashan, 6 km Ghotbravandi Blvd, 8731753153 Kashan, Iran.
Email: hamed.hashemi@kashanu.ac.ir, hhashemi@fel.zcu.cz

Abstract

The optimized protective systems for smart grids and microgrids have received much attention in recent years. However, besides other selectivity constraints, less attention has been paid to synchronous generators' stability concerns. The stability challenges are intensified in meshed grids compared to radial configurations. The literature review shows that a knowledge gap exists in introducing a communication-aided protective scheme for meshed smart grids, considering the stability constraints. This study tries to fill such a research gap by proposing an optimal protection system using the communication links between directional overcurrent relays on both sides of protection zones/distribution lines. Assigning the optimum standard characteristics to protective relays is another contribution. The introduced study is applied to the distribution portion of the IEEE 30-bus test system. The proposed method is implemented in DIgSILENT and MATLAB to perform the power system simulations and solve the optimization problem. The comparative test results infer that the proposed communication-aided scheme results in a 49.57% improvement in speed of the protection system, while there is no stability constraint violation compared to conventional communication-free schemes. Test results highlight the advantages of this research to meet the stability constraints of distributed generations and selectivity constraints simultaneously.

1 | INTRODUCTION

In recent years, the deployment of distributed generations (DGs) has increased because DGs result in techno-economic improvements, the capability of distribution networks operating in grid-connected and islanded modes, higher reliability, and power loss decrement [1, 2]. The integration of DGs with distribution networks transforms the structure of these networks into an interconnected active structure [3, 4]. The benefits from DGs could be maximized through the concepts of smart grids and microgrids based on bidirectional energy and data flows [5–7]. The radial architecture of conventional distribution networks is transformed into meshed ones in smart grids, which complicates protection coordination [8, 9]. The interconnected structure of these active networks in the presence of DGs complicates the smart grid's protection designs [10, 11].

Much attention has been paid to optimized protection schemes for smart grids [12]. The optimization problem of protection coordination can be defined as mathematical linear/non-linear problems. It is possible to solve the optimization problem for smart grids' protection as a linear programming (LP) problem, which considers pre-defined pick-up current settings (PCSs) and the time dial settings (TDSs) are optimized [13, 14]. If both TDSs and PCSs are considered to be optimized while the continuous settings are used, the optimization problem would be a non-linear programming (NLP) problem [15, 16]. A mixed-integer NLP (MINLP) problem should be solved the optimization problem of smart grids' protection if both PCSs and TDSs are optimized, and

TABLE 1 Overview of the literature on optimized protection systems for smart grids in the viewpoint of selected optimization algorithms

		Optimization algorithm									
Ref.	Year	Electromagnetic field optimization	Firefly	GA	WCA	Differential evolution (DE)	(PSO)	Interior point method	TLBO	Hybrid algorithms	Other
[28]	2001	×	×	×	×	×	×	×	×	×	×
[29]	2015	×	×	×	×	×	✓	×	×	×	×
[30]	2016	×	×	×	×	×	✓	×	×	×	×
[31]	2017	✓	×	×	×	×	×	×	×	×	×
[32]	2018	×	×	×	×	×	×	×	×	×	×
[33]	2019	×	✓	✓	×	×	×	×	×	×	×
[34]	2019	×	×	✓	×	×	×	×	×	×	×
[20]	2019	×	×	×	✓	×	×	×	×	×	×
[35]	2019	×	×	×	×	×	×	×	×	×	×
[36]	2019	×	×	✓	×	✓	×	×	×	×	×
[37]	2020	×	×	×	✓	×	×	×	×	×	×
[38]	2020	×	×	×	×	×	×	✓	×	×	×
[19]	2020	×	×	×	×	×	✓	×	×	×	×
[25]	2020	×	×	×	×	×	×	×	×	×	×
[23]	2020	×	×	×	×	×	×	×	×	✓	✓
[39]	2020	×	×	×	×	×	✓	×	×	×	×
[24]	2021	×	×	✓	×	×	✓	×	×	×	×
[22]	2021	×	×	✓	×	×	✓	×	✓	×	×
[40]	2021	×	×	✓	×	×	✓	×	×	×	×
[41]	2021	×	×	✓	×	×	✓	×	✓	×	×
[42]	2021	×	×	×	×	×	×	×	×	✓	×
[43]	2021	×	×	✓	×	×	×	×	×	×	×
[44]	2021	×	×	×	×	×	×	×	×	×	✓
Proposed method		×	×	✓	×	×	×	×	×	×	×

at least one set of these settings has been assumed to be discrete [17].

Moreover, several studies have been reported for optimal protection systems for smart grids and distribution networks by meta-heuristic optimization algorithms. Some articles have used one optimization algorithm to solve the problem, such as Genetic Algorithm (GA) [18], Particle Swarm Optimization (PSO) [19], Water Cycle Algorithm (WCA) [20], and Sin-Cos algorithm [21]. Several references have used several optimization algorithms and compared them with each other. For example, Saldarriaga et al. [22] have used GA, PSO, and teaching–learning-based optimization (TLBO) to solve the optimization problem, and the results of each algorithm have been compared. In a series of other articles, such as [23], combining optimization algorithms in hybrid approaches, for example, the GA and PSO, has been reported. In Table 1, the comparison of available research works in the area of optimal protection of smart grids from the viewpoint of optimization algorithm has been presented. The literature review and using a variety of optimization algorithms illustrates the importance of developing an appropriate optimization algorithm improve the performance of solving the optimization problem.

The inverter-based DGs have steadily increased in recent years. However, most of the available DGs, particularly in developing countries, are synchronous generators (SGs) [24]. The SG-based DGs play a crucial role in energy supply and energy system restoration in sensitive areas such as hospital communities and municipal installations [25, 26]. Also, the detailed statistics of Iran's electricity industry for strategic management [27] show that 243 and 270 MW gas-consumer DGs, which are SGs, were installed in 2018 and 2019, respectively. On the other hand, only 100 and 53 MW renewable DGs, which are usually inverter-based DGs, were installed in these two years. The analyses of statistics for DGs in developing countries like Iran can be useful to justify the fact that although inverter-based DGs are steadily increasing, SG-based DGs have a significant share of whole DGs in some areas/countries.

SGs are sensitive to sudden network disturbances due to technical characteristics, for example, low inertia time constants [25, 45, 46]. During significant interruptions, that is, short cir-

TABLE 2 Overview of the literature on optimized protection systems for smart grids in the viewpoint of optimization problem features

		Relay		Type of topology							Relay curves			OF			
Ref.	Year	OCR	DOCR	Radial	Meshed	DG	DG Stability	Voltage Sag	Fault current limiter	Communication	Standard	Non-standard	Smart selection of relay characteristics	Sum of operating time of PRs	Combination of primary, backup DOCRs times and CTI	Sum of operating of PRs and BRs	Multi-objective of DOCRs operating times and other indices
[28]	2001	×	✓	×	✓	×	×	×	×	×	×	×	×	×	×	×	×
[29]	2015	✓	×	×	✓	✓	×	×	✓	×	✓	×	✓	✓	×	×	✓
[30]	2016	×	×	×	✓	×	×	✓	✓	×	×	×	×	×	×	×	✓
[31]	2017	×	✓	×	✓	✓	×	×	×	×	✓	×	×	✓	×	×	×
[32]	2018	×	✓	×	✓	✓	×	×	×	✓	✓	×	×	×	×	✓	×
[33]	2019	✓	×	×	✓	✓	×	×	×	×	✓	×	×	✓	×	×	×
[34]	2019	×	×	✓	×	✓	✓	×	×	×	✓	×	×	×	×	✓	×
[20]	2019	×	✓	×	✓	✓	×	×	×	×	✓	×	×	✓	×	×	×
[35]	2019	✓	×	✓	×	×	×	×	×	×	×	✓	×	✓	×	×	×
[36]	2019	×	✓	×	✓	✓	×	×	×	✓	✓	×	×	×	✓	×	×
[37]	2020	✓	×	✓	×	✓	×	×	×	×	✓	×	×	×	×	✓	×
[38]	2020	×	✓	×	✓	✓	×	×	×	×	✓	×	✓	✓	×	×	×
[19]	2020	×	✓	×	✓	✓	×	×	×	×	✓	×	×	✓	×	×	×
[25]	2020	×	✓	×	✓	✓	✓	×	×	×	✓	×	✓	×	×	✓	×
[23]	2020	×	✓	×	✓	✓	✓	×	×	×	✓	✓	✓	×	✓	×	×
[39]	2020	×	✓	×	✓	✓	×	×	✓	×	✓	×	✓	×	×	✓	✓
[24]	2021	×	✓	✓	×	✓	✓	×	×	×	✓	×	✓	×	×	✓	×
[22]	2021	✓	×	×	✓	✓	×	×	×	×	✓	✓	✓	✓	×	×	×
[40]	2021	×	✓	×	✓	✓	×	×	×	×	✓	×	✓	×	×	✓	×
[41]	2021	×	✓	×	✓	✓	×	×	×	×	×	✓	✓	✓	×	×	×
[42]	2021	×	✓	×	✓	✓	×	×	×	×	✓	×	×	×	×	✓	×
[43]	2021	×	✓	×	✓	✓	×	✓	✓	×	✓	×	✓	✓	×	×	✓
[44]	2021	×	✓	×	✓	✓	×	×	✓	×	✓	×	✓	×	×	✓	✓
Proposed method		×	✓	×	✓	✓	✓	×	×	✓	✓	×	✓	×	×	✓	×

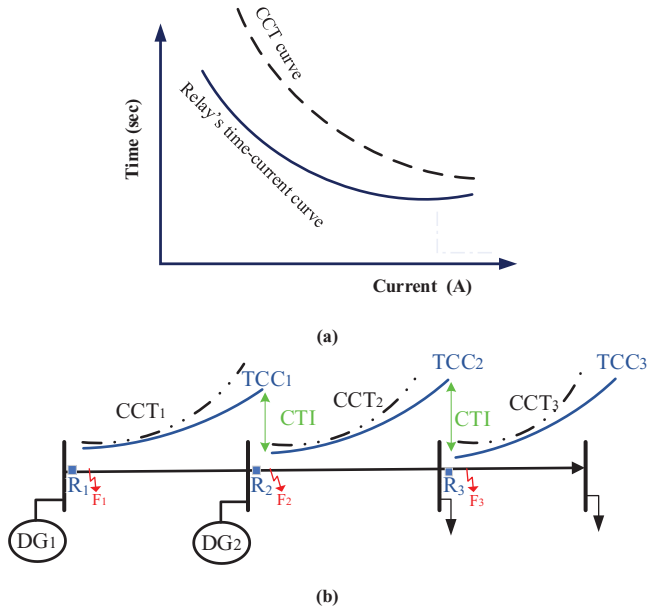

FIGURE 1 Conceptual overview of stability constraints in optimal protection schemes; (a) Faster operating of the protective relays than CCT, (b) Selectivity and stability constraints in radial distribution networks

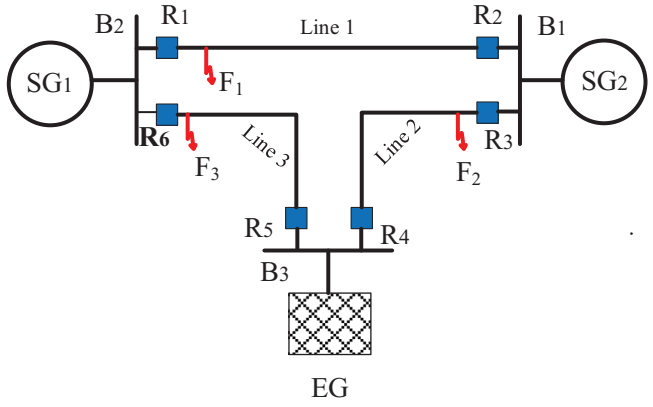

FIGURE 2 A typical ring/meshed distribution system

cuit faults (SCFs), SGs' speed and load angle drastically change [34]. The duration of SCFs and the operating times of protective relays in the network might affect the stability of SGs [47]. If the operating time of the DOCR is more than the critical clearing time (CCT), the SGs will become unstable [48]. The instability of SGs causes problems such as power outages of urban emergency services and the blackout due to cascading events [49]. So it is necessary to consider the transient stability constraints of SGs in the protection schemes.

Although several research works have been developed in optimal protection schemes of smart grids and distribution networks, less attention has been paid to concern the stability constraints of DGs, besides other constraints like selectivity and coordination ones. For instance, Saldarriaga et al. [22] proposed a new optimization problem for protection systems based on standard and non-standard characteristics that neglected the SGs' stability issues. A new solution has been reported in [40] for optimum coordination of directional overcurrent relays (DOCRs) under various configurations. In [36], a new solution was reported based on network status monitoring using communication infrastructures. None of the discussed references in the literature considered the stability constraints in their developed optimal protection schemes.

In a few available references, the stability constraints of SGs have been studied with the reported optimal protection schemes. In [50], new optimal protection coordination was presented based on the DGs' stability constraints. The double-inverse DOCRs were used to implement the proposed optimal protective coordination. Aghdam et al. [34] developed stability-oriented optimization problems using communication systems for the radial grid's protective systems. In addition to optimizing PCSs and TDSs to improve the protection system, one solution is intelligently selecting the characteristic curves for DOCRs [51]. Reference [24] has suggested a solution by optimizing the characteristic curves of DOCRs for the protection problem. In [24], an optimization problem using a double-inverse based on stability constraints in radial distribution networks has been presented. Yazdaninejadi et al. [25] studied the protection problem in ring distribution networks, considering

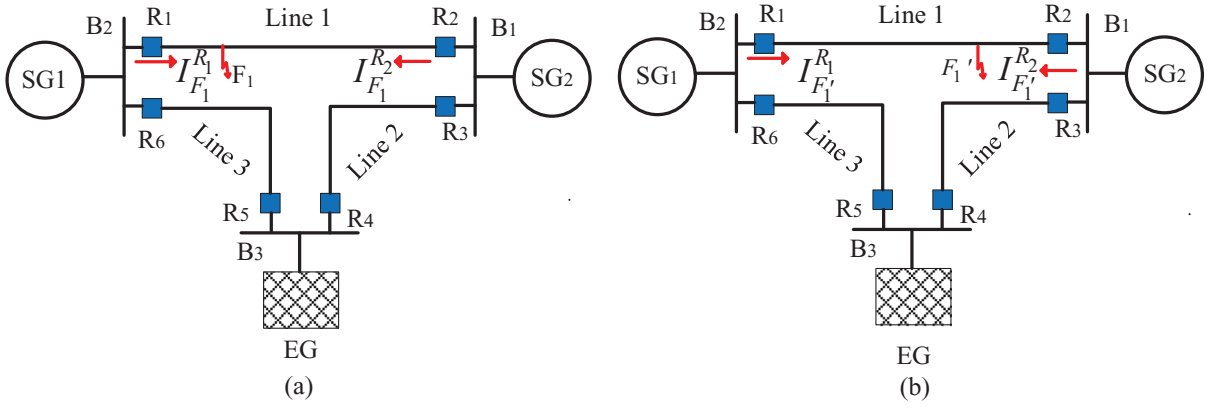

FIGURE 3 SLD of a typical ring/meshed smart grid

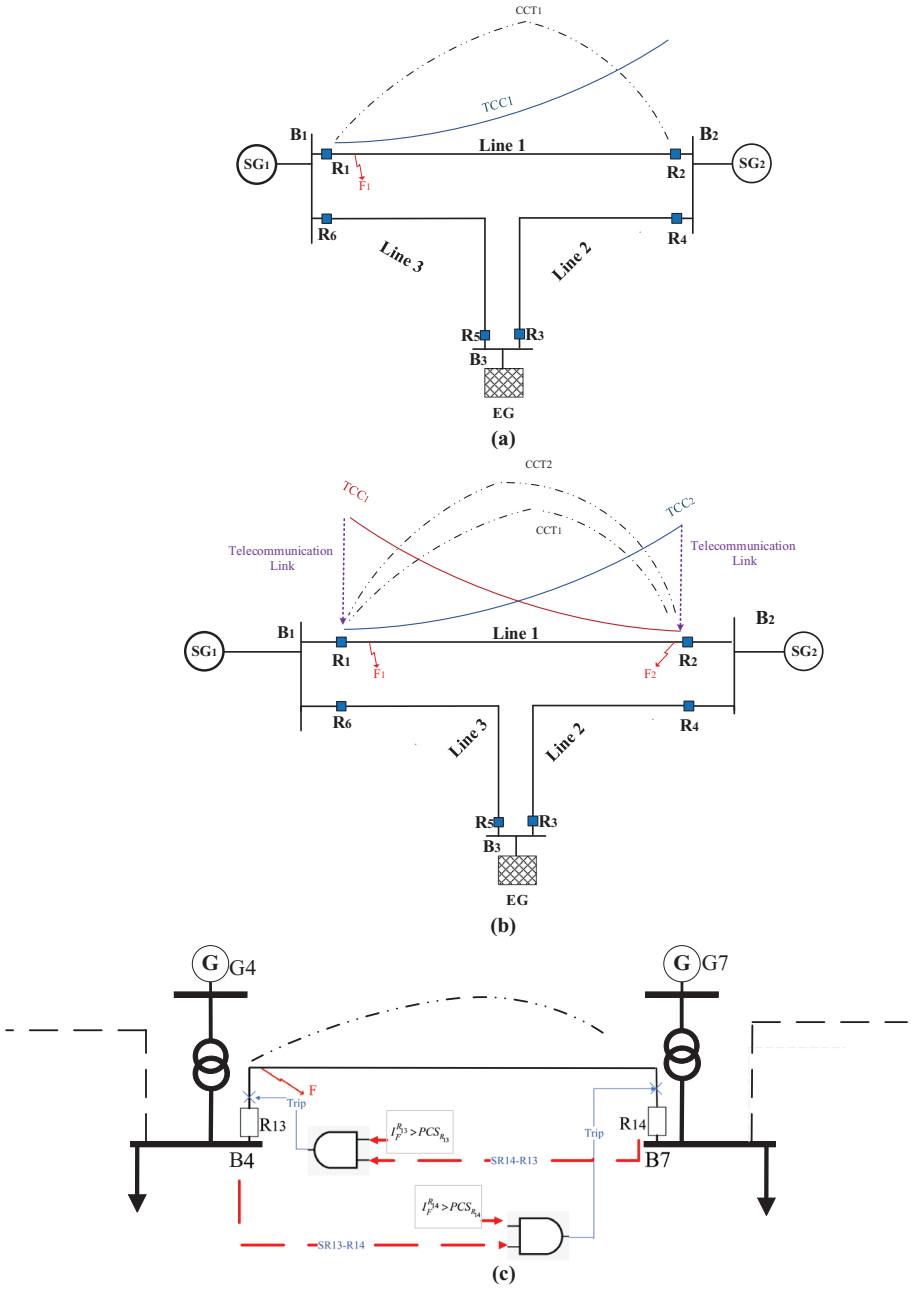

FIGURE 4 Conceptual architecture of the introduced communication-aided protection scheme, considering stability constraints, (a) stability constraint violations in meshed grids by the communication-free scheme, (b) stability constraints satisfaction by the introduced communication-aided scheme, and (c) logic of the proposed scheme using the tripping signal from another side's DOCR

TABLE 3 Standard constants for inverse time-current curves

Item	Curve	A	B	CS
1	NI	0.14	0.02	1
2	VI	13.5	1	2
3	EI	80	2	3

SG stability constraints. The coordination time interval (CTI) and CCT constraints have been satisfied by intelligently selecting the characteristic curves of the relays, besides other decision variables.

Another important feature of available references is their objective function (OF). Different objective functions have been used in existing research works in the optimal protection of smart grids and distribution networks. The total operating time of the primary is one of the well-known objectives, which have been used in some references, that is, [31]. Selecting the total operating time of the primary relays (PRs) and back-up relays (BRs) as the objective function can be seen in others, like [40]. Although these two types of objectives based on the operating time of relays are popular, other combinational objectives, using protective relays' operating time, have been reported. For instance, in [36], the square time of the PRs with

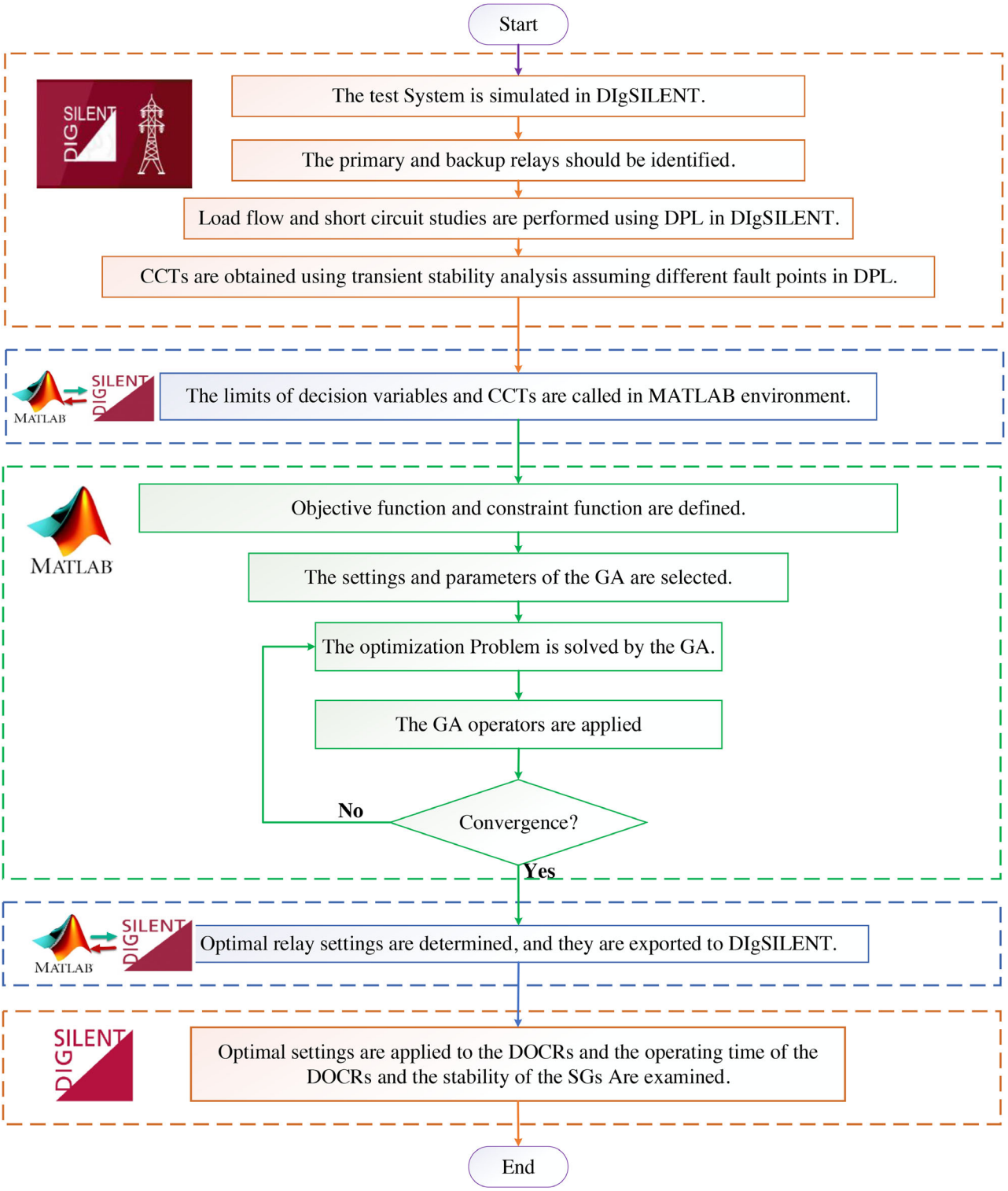

FIGURE 5 Flowchart of the introduced communication-aided protective system according to stability issues of SGs

the square of the difference between the time of the BRs and the coordination time interval have been combined as the objective function [36].

Table 2 summarizes the literature review on protection coordination in smart grids incorporating transient stability of SGs. As can be seen, in most of the available studies, the protective coordination has been done without considering SGs' stability. The literature review shows that although the transient stability of DGs has been considered in some research works, there is a research gap in developing a communication-aided

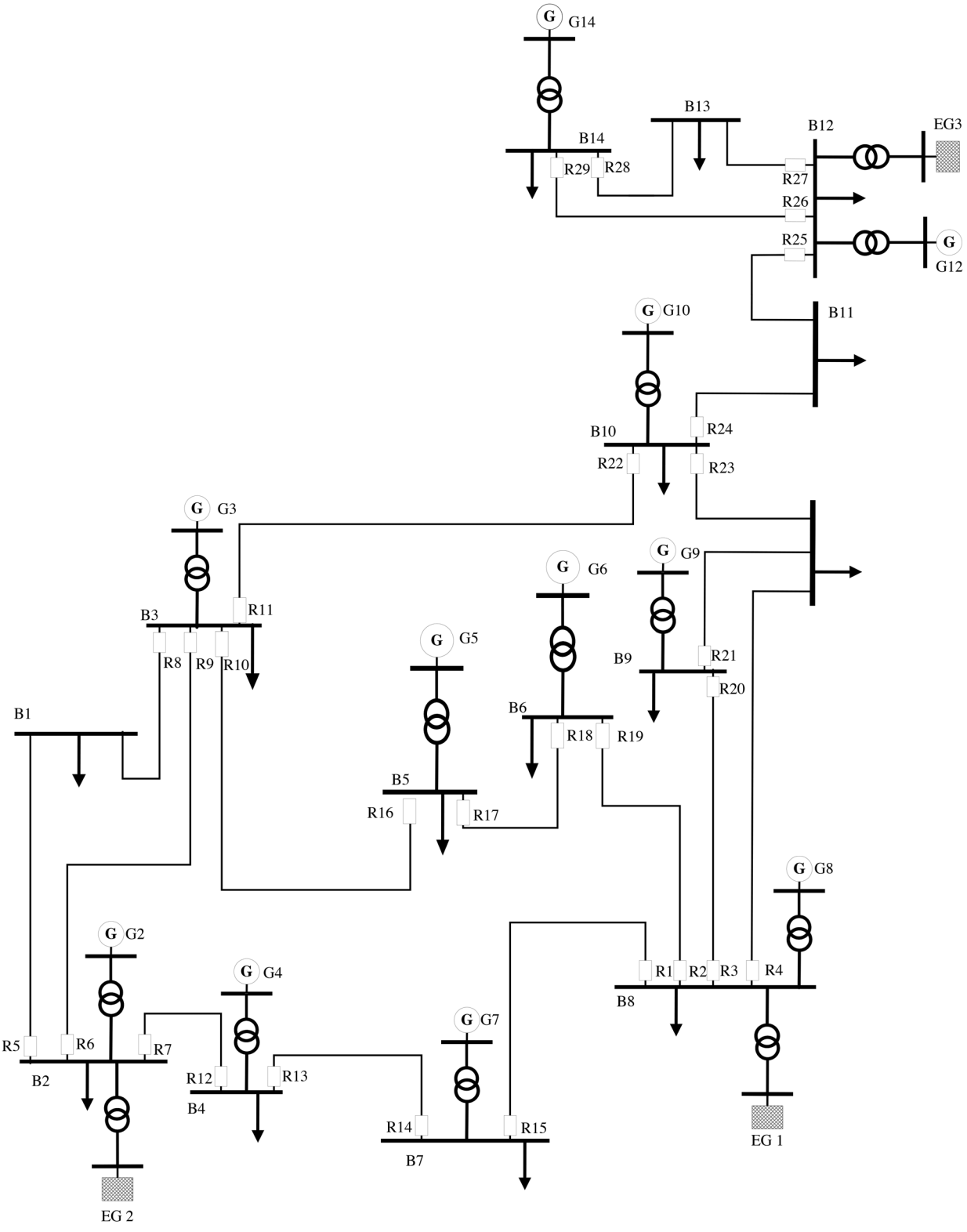

FIGURE 6 Single line diagram (SLD) of the distribution portion of the IEEE 30-bus test system

TABLE 4 Electrical parameters of SGs

Item	Parameter	Value
1	Rated power (MVA)	15
2	Rated power factor	1
3	T_d'(p.u)	0.53
4	T_d''(p.u)	0.03
5	X_d (p.u)	1.5
6	X_d'(p.u)	0.256
7	X_d''(p.u)	0.168
8	X_q(p.u)	0.75
9	X_q''(p.u)	0.184
10	X_l(p.u)	0.2
11	R(p.u)	0

TABLE 5 CTRs

Relay no.	CTR	Relay no.	CTR
1	1000:1	16	500:1
2	800:1	17	800:1
3	800:1	18	800:1
4	1000:1	19	800:1
5	800:1	20	800:1
6	800:1	21	800:1
7	600:1	22	500:1
8	500:1	23	1200:1
9	500:1	24	1200:1
10	500:1	25	1200:1
11	500:1	26	600:1
12	600:1	27	600:1
13	800:1	28	200:1
14	800:1	29	100:1
15	1000:1	–	–

TABLE 6 Short circuit analysis's results of PRs and BRs

Fault location	PR	PR's SCC (kA)	First BR	BR's SCC (kA)	Second BR	BR's SCC (kA)	First BR	BR's SCC (kA)	First BR	BR's SCC (kA)
B_8	R_1	11.84	R_{19}	2.89	R_{20}	1.98	R_{21}	1.19	R_{23}	2.35
B_8	R_2	12.23	R_{15}	3.19	R_{20}	1.98	R_{21}	1.19	R_{23}	2.35
B_8	R_3	13.14	R_{15}	3.19	R_{19}	2.89	R_{21}	1.23	R_{23}	2.36
B_8	R_4	13.71	R_{15}	3.17	R_{19}	2.87	R_{20}	1.91	–	–
B_2	R_5	11.42	R_9	1.23	R_{12}	2.57	–	–	–	–
B_2	R_6	11.53	R_8	1.52	R_{12}	2.51	–	–	–	–
B_2	R_7	10.45	R_8	1.59	R_9	1.25	–	–	–	–
B_3	R_8	7.90	R_6	1.76	R_{16}	2.65	R_{22}	2.56	–	–
B_3	R_9	8.24	R_5	2.19	R_{16}	2.60	R_{22}	2.51	–	–
B_3	R_{10}	7.54	R_5	2.24	R_6	1.77	R_{22}	2.55	–	–
B_3	R_{11}	7.56	R_5	2.24	R_6	1.76	R_{16}	2.63	–	–
B_4	R_{12}	4.72	R_{14}	3.76	–	–	–	–	–	–
B_4	R_{13}	5.42	R_7	4.40	–	–	–	–	–	–
B_7	R_{14}	7.80	R_1	6.85	–	–	–	–	–	–
B_7	R_{15}	4.16	R_{13}	3.17	–	–	–	–	–	–
B_5	R_{16}	5.49	R_{18}	4.51	–	–	–	–	–	–
B_5	R_{17}	4.31	R_{10}	3.31	–	–	–	–	–	–
B_6	R_{18}	8.41	R_2	7.45	–	–	–	–	–	–
B_6	R_{19}	3.82	R_{17}	2.83	–	–	–	–	–	–
B_9	R_{20}	5.67	R_4	2.29	R_{23}	2.76	–	–	–	–
B_9	R_{21}	7.01	R_3	6.07	–	–	–	–	–	–
B_{10}	R_{22}	6.62	R_4	1.39	R_{21}	2.39	R_{25}	2.23	–	–
B_{10}	R_{23}	5.94	R_{11}	2.91	R_{25}	2.24			–	–
B_{10}	R_{24}	7.60	R_4	1.38	R_{11}	2.89	R_{21}	2.38	–	–
B_{12}	R_{25}	8.32	R_{28}	0.22	R_{29}	0.63	–	–	–	–
B_{12}	R_{26}	9.41	R_{24}	1.94	R_{28}	0.20	–	–	–	–
B_{12}	R_{27}	9.63	R_{24}	1.90	R_{29}	0.58	–	–	–	–
B_{14}	R_{28}	3.00	R_{26}	1.92	–	–	–	–	–	–
B_{14}	R_{29}	1.75	R_{27}	0.68	–	–	–	–	–	–

protection scheme, considering the stability constraints to mitigate the challenges in satisfying the stability constraints meshed smart grids.

This research attempts to respond to the gaps by developing a new communication-aided protection scheme for meshed smart grids according to SGs' stability issues. The proposed protective scheme benefits from optimum characteristics assigned for DOCRs and the telecommunication links to communicate between lines' relays.

The proposed method is implemented in the distribution network of the IEEE 30-bus test system. The test system is simulated in DIgSILENT, and load flow, short circuit current (SCC), and CCT results are determined using DIgSILENT Programming Language (DPL). The proposed optimization method is programmed in the MATLAB environment, and the GA solves the optimization problem. The advantages of this research are illustrated compared to available communication-free methods. Moreover, test results imply that optimizing the characteristic curves of DOCRs is an effective solution.

The rest of this article is structured as follows. The problem statement is presented in Section 2. In Section 3, the proposed method, using telecommunication links and intelligent selection of characteristic curves, is reported. Section 4 reports the simulation results, and finally, the conclusion is given in Section 5.

2 | PROBLEM STATEMENT

Although several studies have been reported in the literature in optimal protection systems of smart grids and distribution networks, the stability constraints of synchronous DGs have

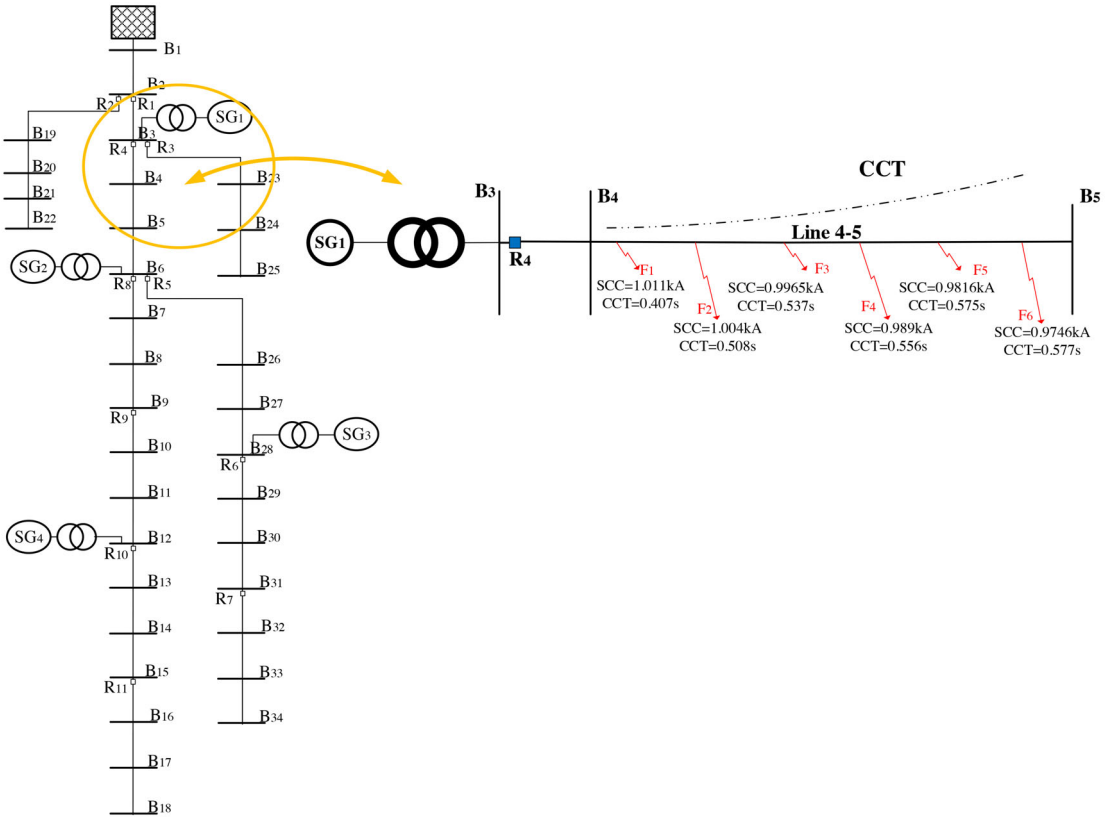

(a) Single line diagram (SLD) of the IEEE 33-bus test system and typical trend of CCT in radial distribution networks and smart grids

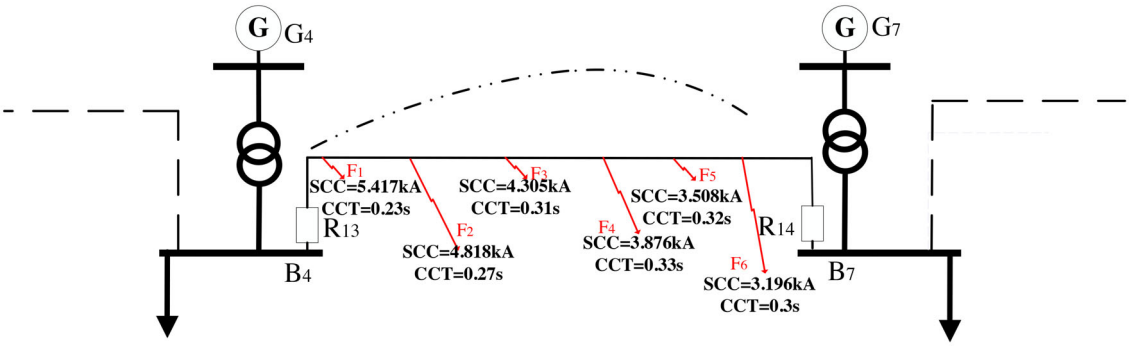

(b) Typical trend of CCT for R_{13} in the distribution portion of IEEE 30-bus test system and typical trend of CCT in meshed networks

FIGURE 7 Typical trends of CCT in radial and meshed distribution networks and smart grids. (a) Single line diagram (SLD) of the IEEE 33-bus test system and typical trend of CCT in radial distribution networks and smart grids. (b) Typical trend of CCT for R_{13} in the distribution portion of IEEE 30-bus test system and typical trend of CCT in meshed networks

received less attention. In Figure 1, the conceptual overview of stability constraints for optimal protection schemes in radial distribution networks has been shown. As depicted, the relays tripping time and their time-current curves (TCCs) for various faults should be less than the related CCT at any fault. Otherwise, at least one DG would be unstable.

The stability concerns and challenges are highlighted in meshed/ring smart grids. In Figure 2, a typical meshed smart grid, including two DGs, is shown. As seen, in the ring and meshed distribution networks, it is essential to operate both protective relays in two ends of faulty areas. Also, the CTI constraints should be satisfied in designing the optimized protective system [52, 53]. As mathematically expressed in (1), the operating time of the BRs should be sufficiently greater than the operating time of the PRs [54, 55]. In the shown typical smart grid, it means that the operating time of relays 1 should be greater than the operating time of relay 3 if a fault occurs in the distribution line, connecting Buses 1 and 3, as described in

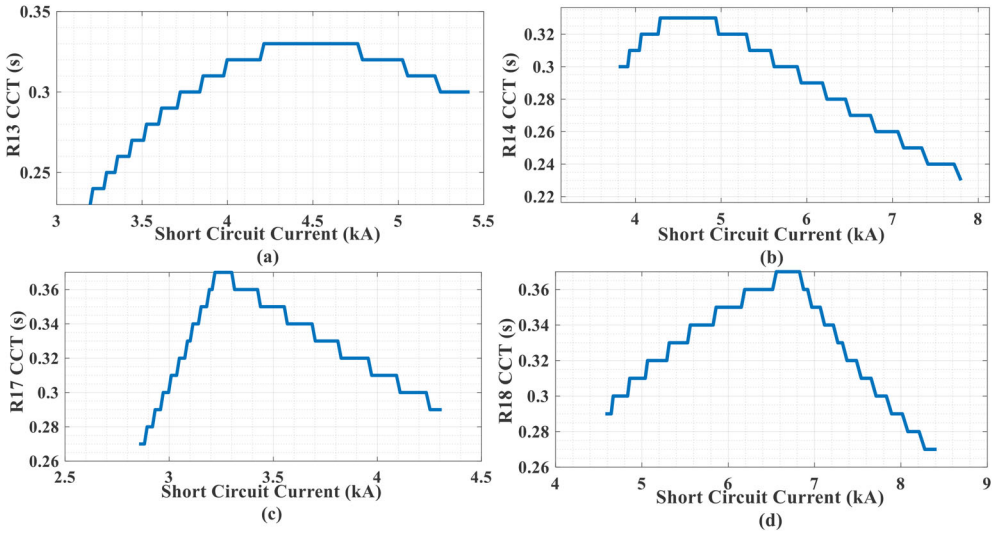

FIGURE 8 CCT curves of typical DOCRs; (a) R_{13}, (b), R_{14}, (c), R_{17}, (d) R_{18}

TABLE 7 The SCC passing through R_4 and its CCT in the IEEE 33-bus test system

PR	Fault location	PR's SCC (kA)	CCT (s)
R_4	F_1-Line$_{4\text{-}5}$	1.0111	0.477
R_4	F_2-Line$_{4\text{-}5}$	1.004	0.508
R_4	F_3-Line$_{4\text{-}5}$	0.9965	0.537
R_4	F_4-Line$_{4\text{-}5}$	0.989	0.556
R_4	F_5-Line$_{4\text{-}5}$	0.9816	0.575
R_4	F_6-Line$_{4\text{-}5}$	0.9746	0.577

TABLE 8 The SCC passing through R_{13} and its CCT in the distribution portion of the IEEE 30-bus test system

PR	Fault location	PR's SCC (kA)	CCT (s)
R_{13}	F_1-Line$_{4\text{-}7}$	5.417	0.23
R_{13}	F_2-Line$_{4\text{-}7}$	4.818	0.27
R_{13}	F_3-Line$_{4\text{-}7}$	4.305	0.31
R_{13}	F_4-Line$_{4\text{-}7}$	3.876	0.33
R_{13}	F_5-Line$_{4\text{-}7}$	3.508	0.32
R_{13}	F_6-Line$_{4\text{-}7}$	3.196	0.3

(2). Similarly, as presented in (3), the time interval between two relays 6 and 2 should be considered.

$$t_{R_j,F_k} > t_{R_i,F_k} + CTI \tag{1}$$

$$t_{R_1,F_2} > t_{R_3,F_2} + CTI \tag{2}$$

$$t_{R_2,F_3} > t_{R_6,F_3} + CTI \tag{3}$$

The CCT constraints should be concerned with the proposed optimization problem to guarantee the stability of SGs. Otherwise, the SGs' stability might be adversely affected due to the slow operating of DOCRs. As shown in (4), to guarantee the stability constraint of SGs, the operating of DOCRs should be less than the minimum CCT [25]. The CCT corresponding to various DGs should be identified, and the minimum CCT would be assigned to the CCT of the understudy relay. For instance, to guarantee the stability constraint of SGs 1 and 2, the operating of R_1 and R_2 should be less than the minimum CCT, as shown in (5) and (6). The CCT corresponding to discussed relays depends on the stability of SG_1 and SG_2, and the minimum CCT based separate SGs should be selected as the CCT.

$$CCT_{R_i,F_k} = Min\left\{CCT_{R_i,F_k}^{SG_1}, CCT_{R_i,F_k}^{SG_2}, \ldots, CCT_{R_i,F_k}^{SG_g}, \ldots, CCT_{R_i,F_k}^{SG_G}\right\} \tag{4}$$

$$CCT_{R_1,F_1} = Min\left\{CCT_{R_1,F_1}^{SG_1}, CCT_{R_1,F_1}^{SG_2}\right\} \tag{5}$$

$$CCT_{R_2,F_1} = Min\left\{CCT_{R_2,F_1}^{SG_1}, CCT_{R_2,F_1}^{SG_2}\right\} \tag{6}$$

The simultaneous satisfaction of CTI and CCT constraints complicates the protection system design. In (7), the stability constraints that should be concerned with the optimal protection scheme of the smart grid are shown.

$$t_{F_k}^{R_1} \le CCT_{F_k}^{R_1} \tag{7}$$

In radial distribution networks, the CCT increases as the fault location moves away from the upstream relay. It means that the CCT increases as the SCC decreases. On the other hand, the slow operating of the DOCR during the low SCCs might not influence the stability of SGs. In radial distribution networks and smart grids, there is no challenge for lower short SCCs if the CCT constraints are satisfied for the maximum SCC.

TABLE 9 Optimal OF values under various scenarios

Scenario no.	Stability constraints	Communication links	OF (s)	Transient stability constraint violations	
Scenario 1	×	×	81.3696	29	All relays
Scenario 2	✓	×	Not feasible	–	–
Scenario 3	×	✓	40.7966	2	R_{13} & R_{17}
Scenario 4 (proposed method)	✓	✓	41.0651	0	0

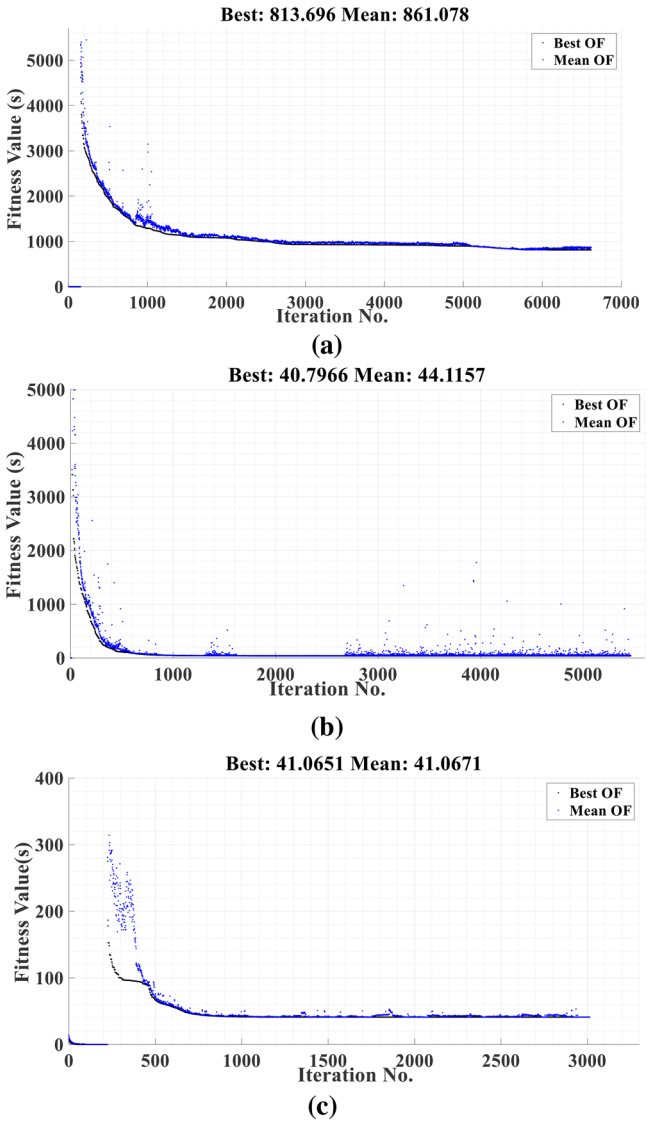

FIGURE 9 Convergence optimization problem solving under (a) Scenario 1; (b) Scenario 3; (c) Scenario 4

On the contrary, in meshed smart grids, the CCT curves would not be strictly decreasing via increasing SCCs. The CCT to guarantee the stability of SGs near to DOCR increases if a fault occurs far from the relay location. But, the CCT corresponding to other DGs connected to the end of the protection zone might decrease. This issue intensifies the challenges in satisfying CCT and CTI constraints simultaneously because the operating time of DOCRs increases via the short circuit decrements, while the CCT might decrease.

TABLE 10 Optimum settings for relays under Scenario 1

Relay no.	I_p (p.u)	*TDS*	Characteristic	Relay no.	I_p (p.u)	*TDS*	Characteristic
R_1	2.9966	0.0820	1	R_{16}	1.1181	0.2349	2
R_2	1.4154	0.3933	3	R_{17}	1.0460	0.3932	1
R_3	1.2693	1.1532	2	R_{18}	1.6408	0.1181	1
R_4	0.3660	0.4194	2	R_{19}	1.1962	0.3718	1
R_5	0.5543	0.4034	3	R_{20}	1.1360	0.2188	2
R_6	0.4603	0.3609	3	R_{21}	0.9435	0.9070	1
R_7	2.0834	0.1910	2	R_{22}	0.6772	0.6359	2
R_8	0.3849	1.2006	2	R_{23}	1.0363	0.3126	2
R_9	0.4319	0.8294	2	R_{24}	1.1460	0.0162	1
R_{10}	1.1348	2.2170	3	R_{25}	1.0788	0.1136	1
R_{11}	0.5741	0.9631	2	R_{26}	0.3821	0.3868	3
R_{12}	1.6196	0.0507	1	R_{27}	0.0634	0.7635	3
R_{13}	1.7252	0.1212	3	R_{28}	0.3980	0.4003	2
R_{14}	1.1362	0.1786	2	R_{29}	2.0927	0.3078	2
R_{15}	1.153509	0.3630103	1	–	–	–	–

For example, as shown in Figure 3, a fault might occur at F_1 or F_1'. The SCC passing through R_1 and R_2 and the operating time of relays and CCTs corresponding to these two fault locations have been compared in (8).

$$\begin{cases} I_{F_1'}^{R_1} \le I_{F_1}^{R_1} \\ CCT_{R_1,F_1'} \le CCT_{R_1,F_1} \end{cases}$$

$$\Rightarrow \begin{cases} t_{F_1'}^{R_1} \ge t_{F_1}^{R_1} \\ t_{F_1'}^{R_1} \ge CCT_{R_1,F_1'} \end{cases} \Rightarrow \text{Stability constraint violation} \quad (8)$$

In practical conditions, it is impossible to speed up the operating time of DOCRs for far-end faults (FEFs) to satisfy the CCT constraints, besides other selectivity and stability constraints. In this paper, a new communication-aided protective scheme, considering stability constraints, is proposed to mitigate the discussed problem, as depicted in Figure 4.

TABLE 11 DOCRs' operating times for NEFs under Scenario 1

PR	Fault location (NEF)	CCT (s)	Tripping time (s)	1st BR	Operating time (s)
R_1	B_8	–	0.4122	R_{19}	2.3299
R_2	B_8	0.25	0.2719	R_{15}	2.4752
R_3	B_8	0.25	1.3038	R_{15}	2.4764
R_4	B_8	0.17	0.1552	R_{15}	2.4911
R_5	B_2	0.31	0.0487	R_9	2.3746
R_6	B_2	0.33	0.0295	R_8	2.3559
R_7	B_2	0.31	0.3501	R_8	2.2391
R_8	B_3	0.29	0.4046	R_6	1.3229
R_9	B_3	0.3	0.3014	R_5	1.3771
R_{10}	B_3	0.3	1.0095	R_5	1.3109
R_{11}	B_3	0.29	0.5130	R_5	1.3167
R_{12}	B_4	0.27	0.2209	R_{14}	0.7700
R_{13}	B_4	0.3	0.6727	R_7	1.0220
R_{14}	B_7	0.23	0.3181	R_1	0.6893
R_{15}	B_7	–	1.9542	R_{13}	2.2641
R_{16}	B_5	0.27	0.3593	R_{18}	0.6616
R_{17}	B_5	0.29	1.6519	R_{10}	5.3801
R_{18}	B_6	0.27	0.4368	R_2	0.7431
R_{19}	B_6	0.29	1.8552	R_{17}	2.2282
R_{20}	B_9	0.27	0.5638	R_4	1.0783
R_{21}	B_9	0.22	2.7848	R_3	3.1259
R_{22}	B_{10}	0.28	0.4625	R_4	2.0271
R_{23}	B_{10}	0.23	1.1167	R_{11}	1.4222
R_{24}	B_{10}	0.28	0.0653	R_4	2.0366
R_{25}	B_{12}	0.32	0.4194	R_{28}	4.0000
R_{26}	B_{12}	0.34	0.0184	R_{24}	0.3295
R_{27}	B_{12}	0.32	0.0010	R_{24}	0.3484
R_{28}	B_{14}	0.35	0.1475	R_{26}	0.4480
R_{29}	B_{14}	0.29	0.5635	R_{27}	4.0000

TABLE 12 DOCRs' operating times in FEF under Scenario 1

PR	Fault location (FEF)	CCT (s)	Operating time (s)	1st BR	Operating time (s)
R_1	B_7	–	0.6771	R_{19}	3.9004
R_2	B_6	0.2900	0.7245	R_{15}	3.8775
R_3	B_9	0.2700	3.0909	R_{15}	3.4588
R_4	B_{10}	0.2300	1.9717	R_{15}	10.4553
R_5	B_3	0.2900	1.2620	R_9	1.5670
R_6	B_3	0.3000	1.2266	R_8	1.5724
R_7	B_4	0.2700	1.0036	R_8	15.7864
R_8	B_2	0.3100	2.1635	R_6	2.8221
R_9	B_2	0.3300	2.1960	R_5	3.0729
R_{10}	B_5	0.2700	5.2547	R_5	5.9874
R_{11}	B_{10}	0.2800	1.3957	R_5	6.7081
R_{12}	B_2	0.3100	0.3523	R_{14}	2.0813
R_{13}	B_7	0.2300	2.2218	R_7	2.5638
R_{14}	B_4	0.3000	0.7571	R_1	5.9865
R_{15}	B_8	–	2.4560	R_{13}	4.8677
R_{16}	B_3	0.3000	0.8296	R_{18}	1.8525
R_{17}	B_6	0.2700	2.2151	R_{10}	14.6070
R_{18}	B_5	0.2900	0.6537	R_2	2.7844
R_{19}	B_8	0.2500	2.3102	R_{17}	3.0275
R_{20}	B_8	0.2500	2.3884	R_4	2.6913
R_{21}	B_8	0.1700	15.8096	R_3	17.7518
R_{22}	B_3	0.2900	1.2796	R_4	10.2083
R_{23}	B_8	0.1700	4.7437	R_{11}	14.9898
R_{24}	B_{12}	0.3200	0.2939	R_4	49.3422
R_{25}	B_{10}	0.2800	1.4176	R_{28}	4.0000
R_{26}	B_{14}	0.2900	0.4244	R_{24}	4.0000
R_{27}	B_{13}	0.3000	0.1860	R_{24}	4.0000
R_{28}	B_{12}	0.3200	2.4953	R_{26}	5.7074
R_{29}	B_{14}	0.3400	1.9333	R_{27}	2.4658

In the proposed protective scheme, if a DOCR trips, a signal sends to another protection side's DOCR. If the other side's DOCR has picked up the short SCC, it operates as receiving a tripping signal. Otherwise, the received signal might be sent due to any noise or interruption. In (9)–(11), the modelling of the proposed communication-aided protection scheme for smart grids is presented. The proposed model would be applicable since the smart grids have been equipped with the required communication infrastructures.

$$S_{R_m,R_n} = \begin{cases} 1 & t \geq t_{F_k}^{R_m} \\ 0 & \text{Otherwise.} \end{cases} \tag{9}$$

$$\xi_{R_n}^{F_k} = \begin{cases} 1 & I_{F_k}^{R_n} \geq PCS_{R_n} \\ 0 & \text{Otherwise.} \end{cases} \tag{10}$$

$$t_{F_k}^{R_n} = \begin{cases} TDS_{R_n} \dfrac{A_{R_n}}{\left(\dfrac{I_{F_k}^{R_n}}{PCS_{R_n}}\right)^{B_{R_n}} - 1} & S_{R_m,R_n} \times \xi_{R_n}^{F_k} = 0 \\ t_{F_k}^{R_m} & S_{R_m,R_n} \times \xi_{R_n}^{F_k} = 1 \end{cases} \tag{11}$$

The proposed protection scheme requires one link between two relays of each protection zone, as depicted in Figure 4c. In Figure 4, it has been shown how the data will be transferred between the relays in the communication-based scheme and its logic. On the other hand, a low bandwidth communication is sufficient to maintain proper protection coordination, considering stability constraints.

It should be noted that besides the advantages of communication-assisted protection schemes, these protection

TABLE 13 Optimal DOCRs' settings under Scenario 3

Relay no.	I_p (p.u)	*TDS*	Characteristic	Relay no.	I_p (p.u)	*TDS*	Characteristic
R_1	1.3762	0.1182	3	R_{16}	1.2446	0.0784	3
R_2	1.7340	0.1418	3	R_{17}	1.0419	0.1038	2
R_3	0.8942	0.4286	3	R_{18}	1.0746	0.1267	3
R_4	0.5260	0.0852	2	R_{19}	1.3714	0.0519	2
R_5	0.3515	0.3293	3	R_{20}	1.1803	0.0191	3
R_6	0.2204	0.5218	3	R_{21}	0.9754	0.0585	1
R_7	1.2623	0.2854	3	R_{22}	0.5924	0.3848	3
R_8	0.8804	0.0810	2	R_{23}	1.0373	0.0408	1
R_9	0.4102	0.1892	3	R_{24}	1.0818	0.0115	2
R_{10}	1.1426	0.2599	3	R_{25}	1.0392	0.0403	1
R_{11}	0.5144	0.7624	3	R_{26}	0.3606	0.3546	3
R_{12}	1.1224	0.0660	2	R_{27}	0.1398	0.2665	3
R_{13}	1.6816	0.0799	1	R_{28}	0.4719	0.0333	1
R_{14}	1.2696	0.0710	3	R_{29}	0.7350	0.2320	3
R_{15}	1.2633	0.0597	1	–	–	–	–

TABLE 14 DOCRs' operating times in NEF under Scenario 3

PR	Fault location (NEF)	CCT (s)	Operating time (s)	1st BR	Operating time (s)
R_1	B_8	–	0.1294	R_{19}	0.4294
R_2	B_8	0.25	0.1478	R_{15}	0.4478
R_3	B_8	0.25	0.1019	R_{15}	0.4481
R_4	B_8	0.17	0.0459	R_{15}	0.4510
R_5	B_2	0.31	0.0160	R_9	0.4298
R_6	B_2	0.33	0.0098	R_8	0.4475
R_7	B_2	0.31	0.1205	R_8	0.4205
R_8	B_3	0.29	0.0645	R_6	0.4235
R_9	B_3	0.3	0.0094	R_5	0.4408
R_{10}	B_3	0.3	0.1200	R_5	0.4201
R_{11}	B_3	0.29	0.0706	R_5	0.4220
R_{12}	B_4	0.27	0.1482	R_{14}	0.4484
R_{13}	B_4	0.3	0.3960	R_7	0.6961
R_{14}	B_7	0.23	0.0980	R_1	0.3980
R_{15}	B_7	–	0.3465	R_{13}	0.6468
R_{16}	B_5	0.27	0.0816	R_{18}	0.3822
R_{17}	B_5	0.29	0.3362	R_{10}	0.6398
R_{18}	B_6	0.27	0.1070	R_2	0.4070
R_{19}	B_6	0.29	0.2828	R_{17}	0.5839
R_{20}	B_9	0.27	0.0435	R_4	0.3436
R_{21}	B_9	0.22	0.1825	R_3	0.4825
R_{22}	B_{10}	0.28	0.0617	R_4	0.7020
R_{23}	B_{10}	0.23	0.1798	R_{11}	0.4798
R_{24}	B_{10}	0.28	0.0321	R_4	0.7059
R_{25}	B_{12}	0.32	0.1459	R_{28}	4.0000
R_{26}	B_{12}	0.34	0.0150	R_{24}	0.3151
R_{27}	B_{12}	0.32	0.0016	R_{24}	0.3337
R_{28}	B_{14}	0.35	0.0652	R_{26}	0.3652
R_{29}	B_{14}	0.29	0.0327	R_{27}	0.3327

systems are affected by communication failures. Hence, it is necessary to study the impact of communication failures on the proposed communication-aided system. Also, proposing some solutions to mitigate the eventual impacts of communication failures on the performance of the introduced protection scheme would be useful.

Redundancy of communication links is one of the solutions to mitigate the negative impacts due to the failure of telecommunication communication. The techno-economic analysis is necessary to investigate the necessity of redundancy in communication links. However, if the redundancy for a telecommunication communication system and its links is not economically feasible, the communication-aided protection system should be adequately robust against the failures in communication links.

Although the proposed communication-aided protection scheme is affected due to failures in communication links, if a failure occurs in the communication system, DOCRs will operate according to their current and time settings. In this case, the near-end fault (NEF) operating time would be satisfying similar to expected performance, while the operating time of DOCRs for FEFs increases due to the failure of telecommunication communication. It means that although the SGs' stability is not guaranteed, the faulty areas are isolated by DOCRs. Besides the proposed protection scheme, the adaptive protection concept of assigning suitable setting groups according to the status of communication links can be studied in future works.

3 | MODELLING AND METHODOLOGY

Several OFs have been proposed for the coordination of DOCRs [23]. The total operating time of the PRs and BRs is one of the well-known objectives for optimal protection of distribution networks and smart grids [3, 31, 56]. In this paper, the total operating time of the PRs and BRs is considered as OF to minimize the operating time of the DOCRs subjects to coordination and transient stability constraints and other technical limits. The mathematical relation of the OF used in this paper is expressed in (12).

$$OF = T\left(CS_r, TDS_r, PCS_r\right) = \left\{ \sum_{i=1}^{N_{PR}} \left(t_i^{NEF}\right) + \sum_{j=1}^{N_{BR}} \left(t_j^{NEF}\right) \right\} \quad \forall r \in \{1, \ldots, N_R\} \tag{12}$$

The variables corresponding to the curve type of DOCRs, TDSs, and PCSs are the decision variables of the proposed

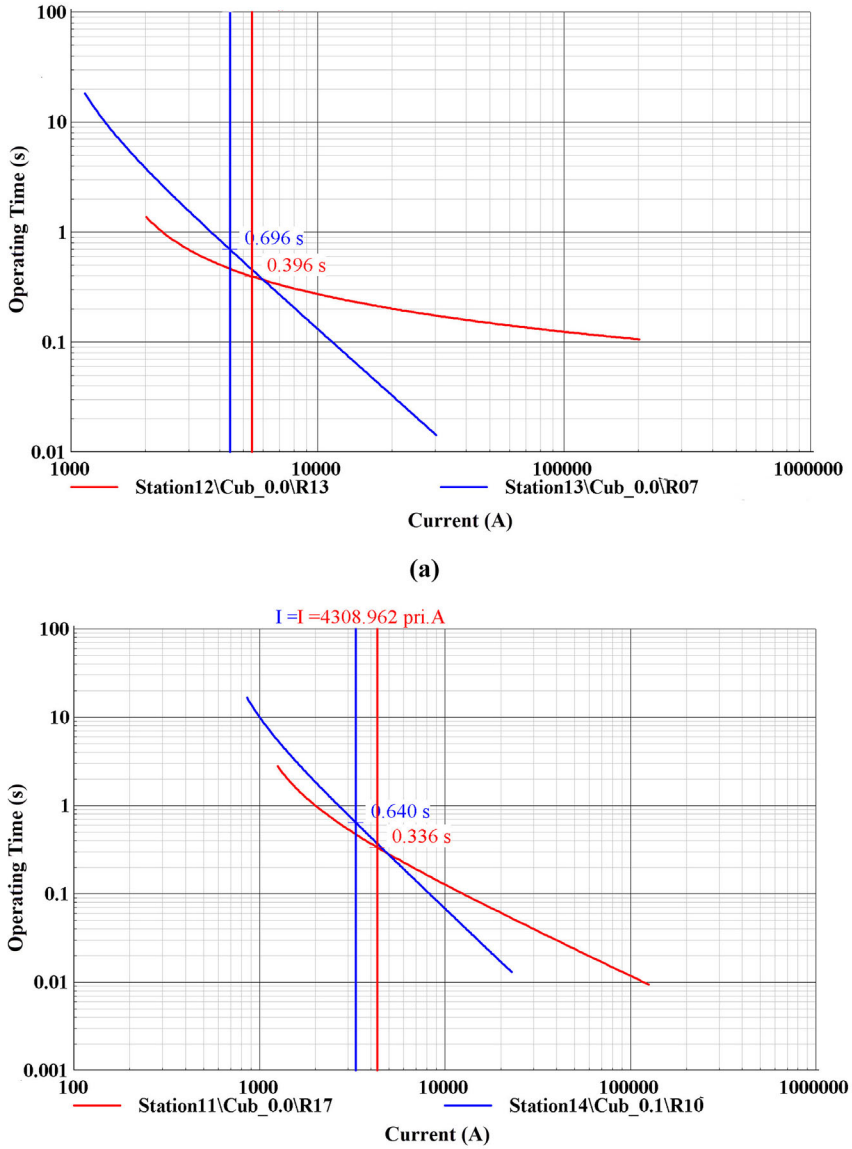

FIGURE 10 Operating time of (a) R_{13}; (b) R_{17} and their back-ups under Scenario 3

optimization problem. An integer variable is assigned to each DOCR, indicating its tripping curve (13). The coefficients of the tripping curves of DOCRs are distinguished based on standard characteristics [57]. The coefficients for standard inverse curves have been demonstrated in Table 3. As seen in (13), CS_r values could be 1, 2, or 3, which represent the normally inverse (NI), very inverse (VI), and extremely inverse (EI) characteristic curves, respectively.

$$\begin{bmatrix} A_r \\ B_r \end{bmatrix} = \begin{cases} \begin{bmatrix} 0.14 \\ 0.02 \end{bmatrix} & CS_r = 1 \\ \begin{bmatrix} 13.5 \\ 1 \end{bmatrix} & CS_r = 2 \\ \begin{bmatrix} 80 \\ 2 \end{bmatrix} & CS_r = 3 \end{cases} \tag{13}$$

As explained in the problem statement, the proposed optimization problem should be solved subject to selectivity and stability constraints. Moreover, other technical limits, such as PCSs and TDSs, should be considered based on relay specifications and other smart grid conditions. The upper and lower bounds of TDSs and PCSs have been described in (14) and (15) [42, 58].

$$TDS^{min} \leq TDS_r \leq TDS^{max} \tag{14}$$

$$PCS_r^{min} \leq PCS_r \leq PCS_r^{max} \tag{15}$$

In this article, the lower and upper limits of TDS are assumed to be 0.01 and 3, respectively. The lower limit of the PCS is considered to be 1.2 times the maximum current transmitting the relay. Also, the upper limit for PCS is the SCC passing through the relays' current transformer in the FEF (minimum SCC).

TABLE 15 Comparison of operating times of R_{13} and R_{17} with CCT under Scenario 3

Fault location	Relay no.	CCT (s)	Operating time (s)	Unstable SGs
B_4	R_{13}	0.3	0.396	All SGs
	R_{14}			
B_5	R_{17}	0.29	0.3362	SG_5
	R_{18}			

The GA is used to solve the optimization problem in the proposed method. Figure 5 shows the flowchart of the proposed method (protection of microgrids, according to SGs' stability concerns using the telecommunication links). First, the studied system is simulated in Digisilent. Afterward, the PRs and BRs are identified, and load flow and short circuit studies with DPL are performed. Moreover, CCTs are extracted using DPL. The load flow and short circuit propagations are used to determine the limits of the DOCRs' current settings. The power flow, short circuit, and CCTs are imported from DIgSILENT to MATLAB. Finally, the optimal settings are extracted, and the operating time of the relays and the transient stability of the SGs are controlled and examined in DIgSILENT.

4 | TEST RESULTS

The proposed method is applied to the distribution portion of the IEEE 30-bus test system, as shown in Figure 6. As can be seen, this test system has 29 DOCRs and 11 SGs. This network's parameters and technical values have been selected based on data reported in [32]. The electrical specifications of all SGs are similar and have been given in Table 4 [32].

Selecting the current transformer ratio (CTR) is one of the essential technical tasks that should be done in designing the protection system of smart grids and microgrids. According to the IEEE Standard C37.110-2007 [59], the CTR shall be selected based on the maximum load current passing through the current transformer (CT). The maximum current in the normal operation of the system must not exceed the CT's rated primary current. The CTR must be large enough so that the secondary current of CT does not exceed 20 times the rated current under the maximum symmetrical primary fault current. The detailed process of CT selection can be seen in a [41]. In this paper, the CTRs have been selected based on the load flow and short circuit analyses and requirements of IEEE Standard C37.110-2007 [59], as presented in Table 5.

The PRs and their BRs, including the SCC passing through the PRs and BRs, have been presented in Table 6.

As discussed, in radial distribution networks and smart grids, if the stability constraints are met corresponding to the

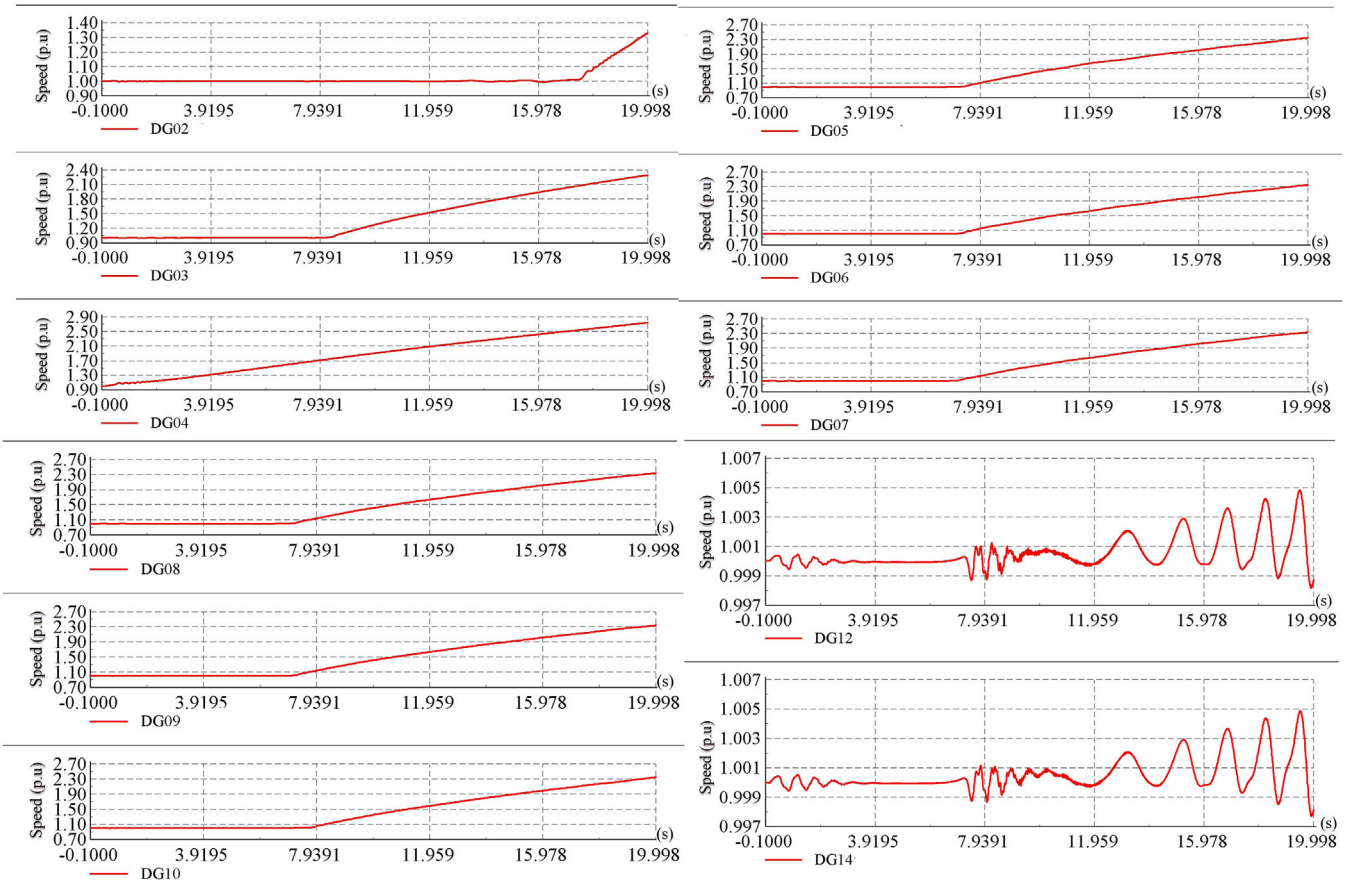

FIGURE 11 Speed of unstable generators after operating of R_{13}

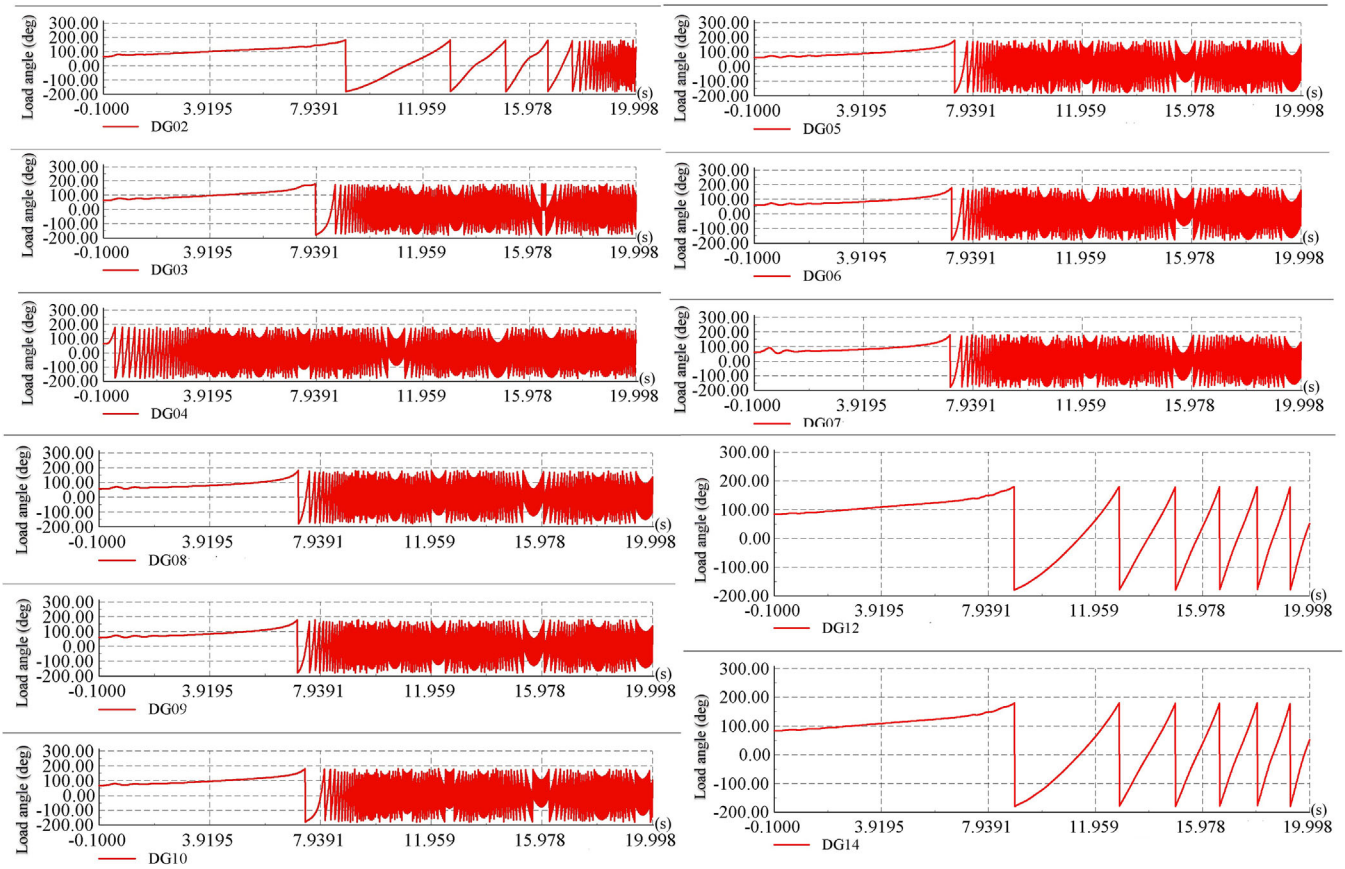

FIGURE 12 Load angle of unstable generators after operating of R_{13}

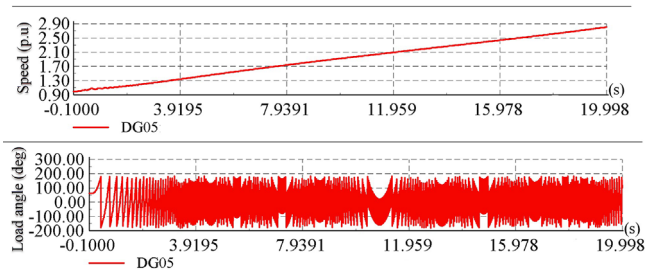

FIGURE 13 Speed and angle of unstable SG5 after operating of R_{17}

maximum fault currents, there is no concern about the CCT constraints satisfaction for lower fault currents. Indeed, the CCT increases as the fault current passing through the DOCR decreases. To illustrate this concept, a typical study has been performed on the IEEE 33-bus test system (radial distribution network), as shown in Figure 7a. In Figure 7 [24], the CCT for the R_4 against the faults at the line connecting buses 4 and 5 are studied. In the IEEE 33-bus test system, when a short circuit occurs downstream of R_4, the stability of SG_1 should be analysed. Table 7 shows the CCT via the SCCs. As can be seen in Figure 7a and Table 7, the CCT increases with increasing the fault distance from R_4 and decreasing the short-circuit current. It is observed that CCT has the lowest/most critical value for the maximum SCC in this condition.

The trend of CCT via the SCC passing through the DOCRs in meshed smart grids is not similar to radial distribution networks. To illustrate the challenges for stability concerns in meshed distribution networks, The CCTs for R_{13} via different faults between the NEFs and FEFs have been shown in Figure 7b. As revealed by results shown in Figure 7b and Table 8, the CCT increases as the fault location moves away from the R13 (F_1–F_4), but this trend changes after F_5, and the CCT values for F_5 and F_6 decrease, while the operating time of R_{13} increase due to SCC decrement. The decrement in CCTs corresponding to F_5 and F_6 appears because of the G_7 stability condition. The typical analyses on radial and meshed smart grids illustrate the discussed challenge about stability-constrained optimal protection systems.

The CCT curves for all DOCRs have been distinguished using the DPL in the DIgSILENT environment. The typical CCT curves for Relays 13, 14, 17, and 18 via SCCs have been shown in Figure 8. As revealed by the CCT curves shown in Figure 8, CCTs are not strictly decreasing via decreasing short-circuit currents in the understudy meshed/ring grid. This behaviour of CCTs results in a faster operating of the relay at the lowest value of short SCC. This is mainly challenging because the operation time of relays increases by decreasing the SCC. However, by using the telecommunication link between the two relays on both sides based on the proposed communication-aided scheme, the DOCR located at the NEF operates faster

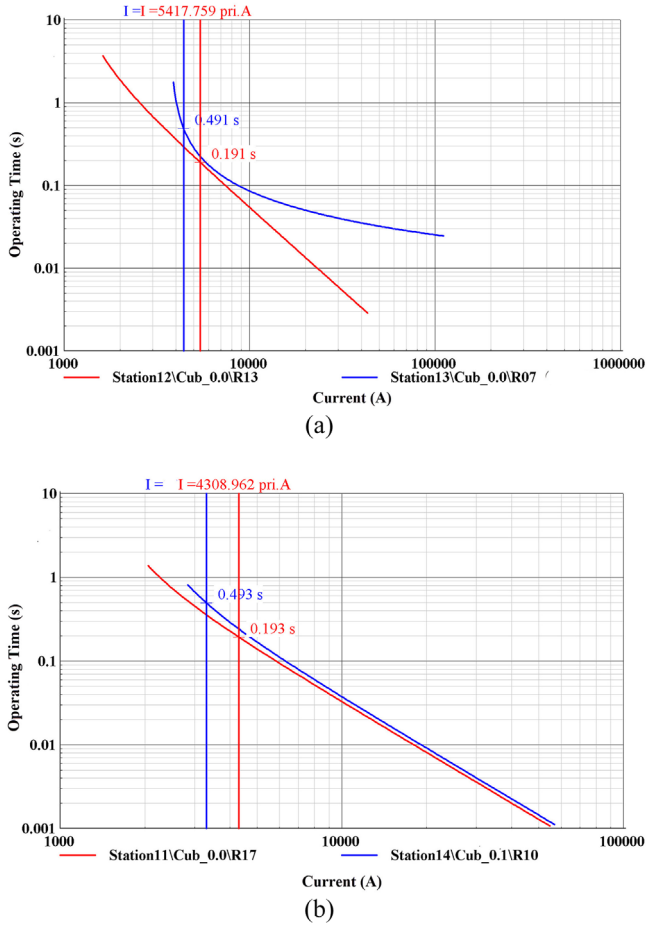

FIGURE 14 Operating time of (a) R_{13}; (b) R_{17} and their back-ups under Scenario 4

TABLE 16 Optimum settings under Scenario 4 (the proposed protection communication-aided scheme, considering stability constraints)

Relay no.	I_p (p.u)	*TDS*	Characteristic	Relay no.	I_p (p.u)	*TDS*	Characteristic
R_1	1.3362	0.1187	3	R_{16}	1.4643	0.0668	2
R_2	1.1570	0.3105	3	R_{17}	1.7101	0.0216	3
R_3	6.3852	0.0118	1	R_{18}	4.8042	0.0100	1
R_4	0.5204	0.0861	2	R_{19}	1.4462	0.0276	3
R_5	0.3840	0.2410	3	R_{20}	1.2290	0.0170	3
R_6	0.2401	0.3843	3	R_{21}	1.1199	0.0535	1
R_7	6.1559	0.0123	1	R_{22}	3.9424	0.0136	1
R_8	2.5570	0.0118	1	R_{23}	1.8046	0.0119	1
R_9	1.2549	0.0141	3	R_{24}	1.1991	0.0153	1
R_{10}	3.7885	0.0126	3	R_{25}	1.4812	0.0126	1
R_{11}	2.9282	0.0141	3	R_{26}	2.3660	0.0160	1
R_{12}	1.1128	0.0544	3	R_{27}	0.8712	0.0124	1
R_{13}	1.3493	0.0577	3	R_{28}	0.4980	0.0351	1
R_{14}	2.0835	0.0198	3	R_{29}	0.8223	0.2013	3
R_{15}	1.0449	0.0673	2	–	–	–	–

TABLE 17 DOCRs' operating times for three-phase NEF under Scenario 4

PR	Fault location (NEF)	CCT (s)	Operating time (s)	1st BR	Operating time (s)
R_1	B_8	–	0.1224	R_{19}	0.4224
R_2	B_8	0.25	0.1431	R_{15}	0.4431
R_3	B_8	0.25	0.0869	R_{15}	0.4434
R_4	B_8	0.17	0.0458	R_{15}	0.4473
R_5	B_2	0.31	0.0140	R_9	0.3932
R_6	B_2	0.33	0.0085	R_8	0.4822
R_7	B_2	0.31	0.0822	R_8	0.3822
R_8	B_3	0.29	0.0444	R_6	0.3710
R_9	B_3	0.3	0.0066	R_5	0.3862
R_{10}	B_3	0.3	0.0680	R_5	0.3680
R_{11}	B_3	0.29	0.0439	R_5	0.3696
R_{12}	B_4	0.27	0.0887	R_{14}	0.3887
R_{13}	B_4	0.3	0.1907	R_7	0.4907
R_{14}	B_7	0.23	0.0758	R_1	0.3758
R_{15}	B_7	–	0.3042	R_{13}	0.6042
R_{16}	B_5	0.27	0.1386	R_{18}	0.4386
R_{17}	B_5	0.29	0.1933	R_{10}	0.4933
R_{18}	B_6	0.27	0.0890	R_2	0.3890
R_{19}	B_6	0.29	0.2236	R_{17}	0.5236
R_{20}	B_9	0.27	0.0421	R_4	0.3421
R_{21}	B_9	0.22	0.1783	R_3	0.4783
R_{22}	B_{10}	0.28	0.0777	R_4	0.6967
R_{23}	B_{10}	0.23	0.0818	R_{11}	0.3818
R_{24}	B_{10}	0.28	0.0633	R_4	0.7006
R_{25}	B_{12}	0.32	0.0562	R_{28}	1.0000
R_{26}	B_{12}	0.34	0.0580	R_{24}	0.3580
R_{27}	B_{12}	0.32	0.0290	R_{24}	0.3819
R_{28}	B_{14}	0.35	0.0697	R_{26}	0.3697
R_{29}	B_{14}	0.29	0.0355	R_{27}	0.3355

than CCT and is connected with the DOCR located on the FEF, and the fault is eliminated properly.

In this article, four scenarios are followed to determine the benefits of this research:

- Scenario 1: The SG's stability constraints are not considered in Scenario 1. Also, the smart grid's protection scheme has not been equipped with a communication system. Hence, the settings of DOCRs are optimized for NEFs and FEFs.
- Scenario 2: In this case, the constraints of the stability of the SGs are considered in the protection scheme. But, telecommunication links are not used. In this scenario, in addition to detecting far-end and NEFs, the DOCRs must operate less than the CCTs.

- Scenario 3: In this scenario, the stability constraints of the SGs are not considered, while telecommunication links are used to connect the relays on both sides of the protection zones. DOCRs detect NEFs, sending a signal to the opposite relay. Finally, the faulty area is isolated from the network using the communication-aided protection scheme.
- Scenario 4: In this scenario (the proposed method), the stability constraints of SGs are considered while telecommunication links are used. Therefore, the DOCRs detect NEFs in this scenario, connecting to the opposite relay. Hence, both relays at two ends of protection zones should operate faster than CCT at the same time.

Test results infer no feasible solution under Scenario 2, highlighting the importance of solutions to meet coordination and stability constraints simultaneously. Also, the convergence diagrams of solving the optimization problem by the GA under various scenarios (except Scenario 2) are shown in Figure 9.

Table 9 shows the optimal values of the OF under different scenarios. As can be seen, the operating times of all DOCRs are greater than the CCTs under Scenario 1. It is concluded that for meshed smart grids and discussed challenges of CCTs for low SCCs passing through the DOCRs, the stability constraint violations have been highlighted compared to radial networks.

Another result that claims attention is the advantages of the proposed communication-aided protection scheme under Scenario 3 compared to Scenario 1. Test results imply that 49.86% improvement in the total operating time of protective relays could be achievable by implementing the communication-aided scheme. The communication system and operating of DOCRs based on received signals from other ends of protection zones improve the stability constraints under scenario 3. However, there are 2 stability constraint violations under Scenario 3. As revealed by test results shown in Table 9, the operating times of relays 13 and 17 are slower than required CCTs. Hence, the SGs would be unstable if a fault occurs downstream of these two DOCRs.

Test results under Scenario 4 (proposed method), considering stability constraints using the communication system, show that the stability of all SGs is guaranteed. Moreover, the speed of the protection scheme is desired under Scenario 4. The total operating time of the DOCRs in the proposed method has increased by 0.658% compared to the third scenario because of SGs' stability constraints. Optimization results emphasize the benefits and usefulness of this study.

Table 10 presents the settings of DOCRs under the first scenario. These settings have been applied to the relays in the DIgSILENT software, and the operating time of the DOCRs has been obtained.

In all scenarios, the objective function of the optimization problem has been defined according to NEFs. However, in test results and discussions, the operating times of DOCRs at NEFs and FEFs have been discussed. The FEFs are important under Scenarios 1 and 2 because the DOCRs operating times are different for NEFs and FEFs. On the contrary, under Scenarios 3 and 4, there is a communication link between two DOCRs on two sides of protection zones, and both relays operate simultaneously. Indeed, the FEF of each DOCR is the NEF of another side's relay in the proposed protection scheme.

TABLE 18 Comparison of R_{13} and R_{17} operating times with CCT under Scenario 4

Fault location	Relay no.	CCT (s)	Operating time (s)
B_4	R_{13}	0.3	0.191
	R_{14}		
B_5	R_{17}	0.29	0.193
	R_{18}		

Tables 11 and 12 show the operating times of the relays at NEFs and FEFs, respectively. As revealed by test results shown in Tables 11 and 12, the CTI constraints have been met. Most operating times of relays are lower than CCT at NEFs, but at FEFs, operating times of several relays are higher than CCT. It means that the faulty line has not been isolated from the network at the right time and at least one of the SGs becomes unstable. As can be seen, violations of the constraints related to the stability of SGs occur in FEFs. The first scenario results show that it is inevitable to concern the CCT constraints, besides selectivity constraints. Moreover, several BRs operating times are more than two seconds under Scenario 1. Indeed, the back-up protection under Scenario 1 would be ineffective in some cases.

As discussed, under Scenario 3, telecommunication links are used, while the stability constraints of SGs are not considered. In the proposed communication-aided protection scheme, the relays operate in NEF using the telecommunication link and are linked to the opposite relay. It means that the relays operate in FEF simultaneously with the near-end relay through the telecommunication links.

The optimized settings of DOCRs under Scenario 3 have been presented in Table 13. Table 14 shows the operating times of the primary DOCRs and their first BRs. As expected, all CTI constraints between the main and BRs have been satisfied. Also, in this scenario, the operating times of any BR do not exceed two seconds. The communication-aided protection scheme has improved the speed of the understudy smart grid and back-up protections. However, the results show two violations of the stability constraint occur under Scenario 3. Significant reduction of the total operating time of relays, mitigating the blind spots' protection, and the low number of violations of the SGs' stability constraint illustrate the advantages of telecommunication links.

The operating times of the relays in Table 14 belong to NEFs. Obviously, due to the use of the telecommunication links, the operating time of the DOCRs in the FEF is equal to the opposite DOCR's operating time, which is at its NEF.

As can be seen in Table 14, only the operating times of R_{13} and R_{17} are higher than corresponding CCTs. The obtained optimized settings under Scenario 3 have been applied to DIgSILENT simulations. Figure 10 shows the time-current characteristics and the operating time of these two relays and their BRs based on DIgSILENT protection simulations. As

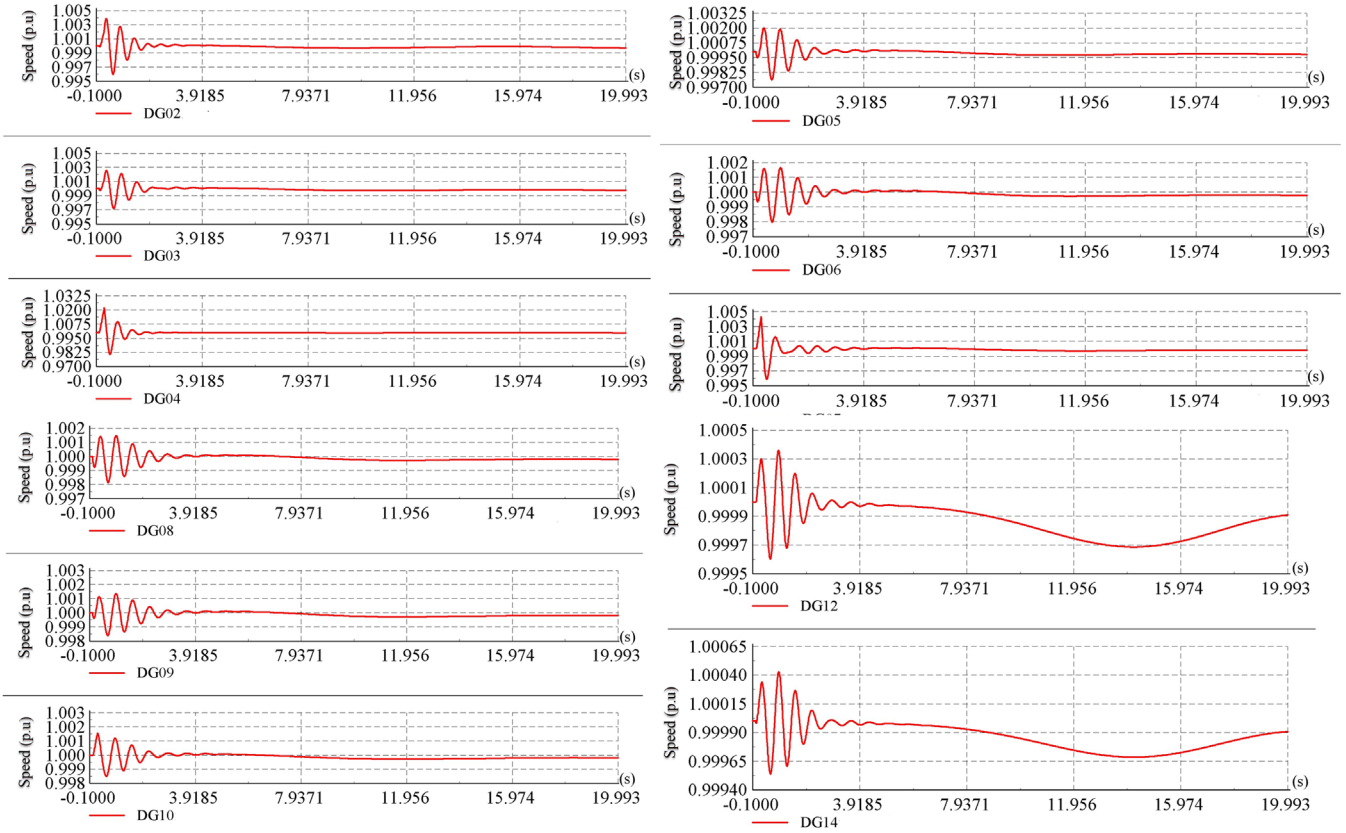

FIGURE 15 Speed of stable generators after operating of R_{13} under Scenario 4

shown in Figure 10, a sufficient time interval exists between the operating time of these relays.

Table 15 shows the unstable SGs due to the operating time of R_{13} and R_{17} that are more than CCTs. Figures 11 and 12 show the speed and load angle of unstable generators due to slow operating of R_{13}, respectively. Also, Figure 13 shows the speed and load angle of unstable generators after R_{17} operation. As revealed by test results shown in Figure 13, only SG5 would be unstable due to the slow tripping of R_{17}.

In the proposed method, considering stability constraints, although increasing the total operating time of the relays, none of the selectivity and stability constraints is violated. Table 16 shows the optimal settings for DOCRs under Scenario 4 (the proposed communication-aided scheme, considering stability constraints). In addition, Table 17 presents the main relays' operating times and their first BRs. As can be seen, in addition to the CTI satisfaction between the PRs and their back-ups, none of the operating time of DOCRs has exceeded the CCT. In the following, the operating time of R_{13} and R_{17} and the stability of the generators are examined compared to Scenario 3.

Figure 14 shows the operating time of R_{13} and R_{17} and the operating time of their BRs based on DIgSILENT simulations and optimized settings under Scenario 4. In Table 18, the operating times of R_{13} and R_{17} have been compared with CCTs. The operating times of these relays are less than CCT, so by detecting the fault and connecting to the opposite relay, the faulty line is isolated. For instance, when a fault occurs near the R_{13}, this relay operates 0.191 seconds after the fault, which is less than its CCT (0.3 s). Moreover, a signal is sent to another side of the faulty area (R_5), and the fault line is isolated from the circuit after 0.191 s.

In Figures 15 and 16, the speed and load angle of the SGs are depicted after R_{13} operating, respectively. Also, Figure 17 shows the speed and load angle of SG_5 after R_{17} operating. Test results infer that, unlike Scenario 3, none of the generators would be unstable under Scenario 4.

The comparative test results highlight the advantages of the proposed communication-aided scheme, considering stability constraints in meshed smart grids. The simultaneous optimal selection of relay characteristics and communication links improves the speed of the protection scheme, while no selectivity and stability appear.

The comparative test results imply that a 49.57% improvement in smart grids' protection system has been obtained compared to conventional communication-free protection schemes, neglecting the stability constraints. In addition, mitigating the SGs' stability challenges compared to approaches, neglecting the stability constraints has been emphasized.

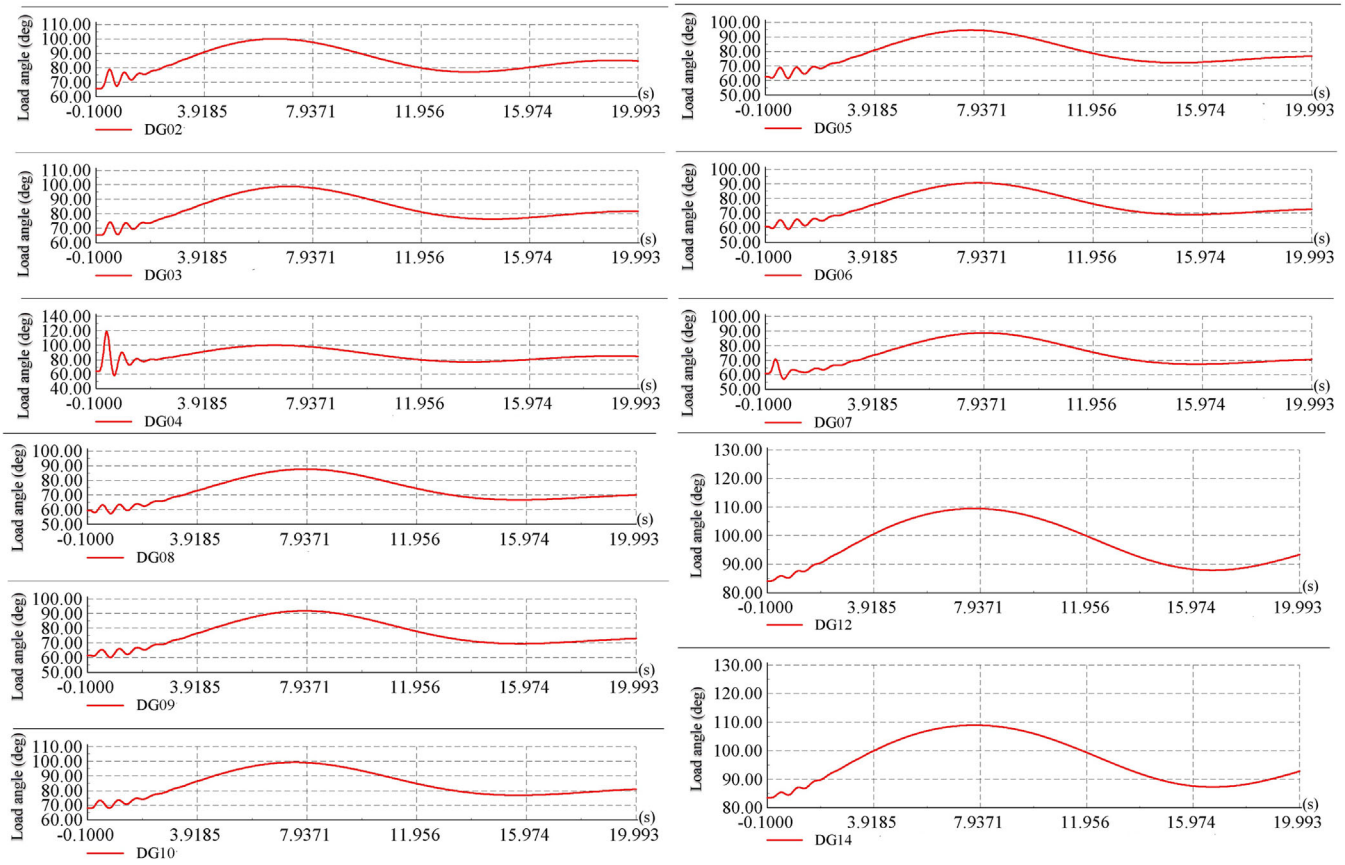

FIGURE 16 Load angle of stable generators after operating of R_{13} under Scenario 4

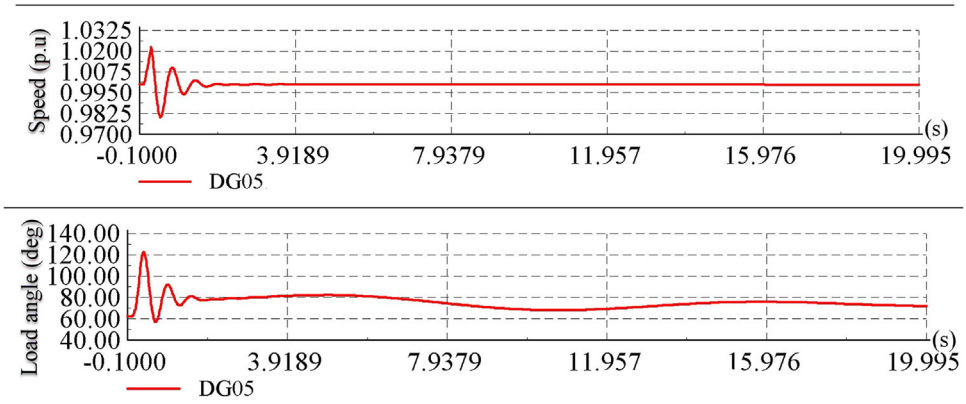

FIGURE 17 Speed and load angle of stable SG_5 after operating of R_{17} under Scenario 4

Furthermore, it is useful to discuss how the coordination will be maintained under different types of faults such as line-to-line (LL) and line-to-line to the ground (LLG). Hence, the LL and LLG SCCs are presented in Tables 19 and 20, respectively. Also, the operating time of PRs and BRs and stability constraints satisfaction against the LL and LLG faults have been studied under Scenario 4 (the proposed method).

Test results show that the coordination will be maintained under different types of faults, for example, LL and LLG, as shown in Tables 21 and 22. Moreover, the stability constraints will be satisfied during the LL and LLG faults based on the obtained optimal settings in the proposed communication-aided scheme. However, some LL and LLG are not detected by the back-up protection, and additional solutions should be considered for these conditions.

TABLE 19 The SSC passing through the DOCRs in LL faults

Fault location	PR	PR's SCC (kA)	First BR	BR's SCC (kA)
B_8	R_1	9.729	R_{19}	2.77
B_8	R_2	10.097	R_{15}	2.801
B_8	R_3	10.975	R_{15}	3.089
B_8	R_4	11.555	R_{15}	3.065
B_2	R_5	9.95	R_9	1.008
B_2	R_6	9.991	R_8	1.249
B_2	R_7	9.231	R_8	1.308
B_3	R_8	6.716	R_6	1.567
B_3	R_9	7.008	R_5	1.965
B_3	R_{10}	6.68	R_5	2.01
B_3	R_{11}	6.431	R_5	2.006
B_4	R_{12}	3.808	R_{14}	2.874
B_4	R_{13}	4.949	R_7	4.011
B_7	R_{14}	6.34	R_1	5.47
B_7	R_{15}	3.919	R_{13}	3.033
B_5	R_{16}	4.485	R_{18}	3.551
B_5	R_{17}	3.971	R_{10}	3.052
B_6	R_{18}	6.887	R_2	6.024
B_6	R_{19}	3.574	R_{17}	2.712
B_9	R_{20}	5.15	R_4	1.786
B_9	R_{21}	5.713	R_3	4.932
B_{10}	R_{22}	5.746	R_4	1.001
B_{10}	R_{23}	5.579	R_{11}	2.441
B_{10}	R_{24}	6.029	R_4	0.996
B_{12}	R_{25}	7.667	R_{28}	0.2
B_{12}	R_{26}	8.081	R_{24}	1.154
B_{12}	R_{27}	8.293	R_{24}	1.124
B_{14}	R_{28}	2.562	R_{26}	1.636
B_{14}	R_{29}	1.497	R_{27}	0.584

TABLE 20 The SSC passing through the DOCRs in LLG faults

Fault location	PR	PR's SCC (kA)	First BR	BR's SCC (kA)
B_8	R_1	11.342	R_{19}	2.857
B_8	R_2	11.611	R_{15}	3.125
B_8	R_3	12.654	R_{15}	3.124
B_8	R_4	13.252	R_{15}	3.106
B_2	R_5	10.866	R_9	1.265
B_2	R_6	10.937	R_8	1.565
B_2	R_7	9.907	R_8	1.633
B_3	R_8	7.825	R_6	1.667
B_3	R_9	8.179	R_5	2.085
B_3	R_{10}	7.29	R_5	2.135
B_3	R_{11}	7.392	R_5	2.131
B_4	R_{12}	4.88	R_{14}	3.732
B_4	R_{13}	5.257	R_7	4.233
B_7	R_{14}	7.689	R_1	6.638
B_7	R_{15}	4.08	R_{13}	3.093
B_5	R_{16}	5.563	R_{18}	4.448
B_5	R_{17}	4.263	R_{10}	3.235
B_6	R_{18}	8.203	R_2	7.157
B_6	R_{19}	3.784	R_{17}	2.801
B_9	R_{20}	5.495	R_4	2.195
B_9	R_{21}	6.848	R_3	5.874
B_{10}	R_{22}	6.466	R_4	1.351
B_{10}	R_{23}	5.749	R_{11}	2.881
B_{10}	R_{24}	7.632	R_4	1.346
B_{12}	R_{25}	7.828	R_{28}	0.253
B_{12}	R_{26}	8.778	R_{24}	1.975
B_{12}	R_{27}	9.063	R_{24}	1.942
B_{14}	R_{28}	2.964	R_{26}	1.83
B_{14}	R_{29}	1.819	R_{27}	0.649

5 | CONCLUSION

This study has tried to fill the research gaps in the optimal protection system of meshed smart grids, considering the stability constraints by proposing a new communication-aided scheme. In the proposed research, the DOCRs of both sides of distribution lines/protection zones are connected through a communication link. The proposed communication-aided protection scheme is a suitable solution to mitigate the challenges regarding the stability constraints of FEFs in meshed smart grids.

The introduced method has been applied to the distribution portion of the IEEE 30-bus test system. Test results under various scenarios illustrated the advantages of the proposed method. The comparative results have illustrated that the stability concerns are emphasized in meshed smart grids, and it is inevitable to find a solution to respond to these problems. It has been concluded that the proposed communication-aided protection system would be desired based on SGs' stability constraints, even by determining the optimal relay settings without consideration of stability constraints (Scenario 3). This is mainly because of the fast operating of DOCRs for FEFs by sending/receiving communication links from the other side of the protection zone, which corresponds to a NEF. The comparative test results show that a 49.57% decrement in operating times of DOCRs has been achieved compared to conventional communication-free protection schemes, neglecting the stability constraints. Furthermore, mitigating the SGs' stability challenges by the proposed method compared to approaches, neglecting the stability constraints has been highlighted.

TABLE 21 DOCRs' operating times for LL NEF under Scenario 4

PRs	Fault location (NEF)	CCT (s)	Operating time (s)	1st BR	Operating time (s)
R_1	B_8	–	0.182504	R_{19}	0.479266
R_2	B_8	0.25	0.210499	R_{15}	0.540383
R_3	B_8	0.25	0.107545	R_{15}	0.464247
R_4	B_8	0.17	0.054801	R_{15}	0.469762
R_5	B_2	0.31	0.018394	R_9	0.713652
R_6	B_2	0.33	0.011368	R_8	–
R_7	B_2	0.31	0.093466	R_8	3.605477
R_8	B_3	0.29	0.048855	R_6	0.469012
R_9	B_3	0.3	0.009117	R_5	0.482976
R_{10}	B_3	0.3	0.088329	R_5	0.461081
R_{11}	B_3	0.29	0.061633	R_5	0.462966
R_{12}	B_4	0.27	0.137924	R_{14}	0.803031
R_{13}	B_4	0.3	0.230381	R_7	1.047072
R_{14}	B_7	0.23	0.117645	R_1	0.602398
R_{15}	B_7	–	0.330179	R_{13}	0.668938
R_{16}	B_5	0.27	0.175815	R_{18}	–
R_{17}	B_5	0.29	0.232211	R_{10}	0.632925
R_{18}	B_6	0.27	0.119785	R_2	0.600587
R_{19}	B_6	0.29	0.25884	R_{17}	0.588536
R_{20}	B_9	0.27	0.051414	R_4	0.477784
R_{21}	B_9	0.22	0.198502	R_3	–
R_{22}	B_{10}	0.28	0.088176	R_4	1.258113
R_{23}	B_{10}	0.23	0.087296	R_{11}	0.633545
R_{24}	B_{10}	0.28	0.073699	R_4	1.271338
R_{25}	B_{12}	0.32	0.059349	R_{28}	4
R_{26}	B_{12}	0.34	0.063193	R_{24}	–
R_{27}	B_{12}	0.32	0.030566	R_{24}	–
R_{28}	B_{14}	0.35	0.073214	R_{26}	0.787103
R_{29}	B_{14}	0.29	0.048741	R_{27}	0.782405

TABLE 22 DOCRs' operating times for LLG NEF under Scenario 4

PRs	Fault location (NEF)	CCT (s)	Operating time (s)	1st BR	Operating time (s)
R_1	B_8	–	0.133607	R_{19}	0.433744
R_2	B_8	0.25	0.158854	R_{15}	0.456212
R_3	B_8	0.25	0.090539	R_{15}	0.456431
R_4	B_8	0.17	0.047496	R_{15}	0.460417
R_5	B_2	0.31	0.015421	R_9	0.368121
R_6	B_2	0.33	0.009486	R_8	0.406668
R_7	B_2	0.31	0.08671	R_8	0.385854
R_8	B_3	0.29	0.044665	R_6	0.413695
R_9	B_3	0.3	0.006679	R_5	0.427784
R_{10}	B_3	0.3	0.073139	R_5	0.407563
R_{11}	B_3	0.29	0.046038	R_5	0.409127
R_{12}	B_4	0.27	0.082954	R_{14}	0.394808
R_{13}	B_4	0.3	0.203023	R_7	0.632953
R_{14}	B_7	0.23	0.078129	R_1	0.400892
R_{15}	B_7	–	0.312664	R_{13}	0.639672
R_{16}	B_5	0.27	0.136582	R_{18}	0.480314
R_{17}	B_5	0.29	0.197962	R_{10}	0.527038
R_{18}	B_6	0.27	0.091995	R_2	0.422506
R_{19}	B_6	0.29	0.228027	R_{17}	0.540197
R_{20}	B_9	0.27	0.044953	R_4	0.361094
R_{21}	B_9	0.22	0.180486	R_3	0.592437
R_{22}	B_{10}	0.28	0.079319	R_4	0.727995
R_{23}	B_{10}	0.23	0.084587	R_{11}	0.392573
R_{24}	B_{10}	0.28	0.063134	R_4	0.732403
R_{25}	B_{12}	0.32	0.058505	R_{28}	4.000
R_{26}	B_{12}	0.34	0.060273	R_{24}	0.367203
R_{27}	B_{12}	0.32	0.029588	R_{24}	0.356216
R_{28}	B_{14}	0.35	0.069966	R_{26}	0.439274
R_{29}	B_{14}	0.29	0.03298	R_{27}	0.40049

NOMENCLATURE

Indices

- r Index of relay ($r = 1 : N_R$)
- i Index of primary relay ($i = 1 : N_{PR}$)
- j Index of back-up relay ($j = 1 : N_{BR}$)
- n Index of the relay at sending side of the communication link ($n = 1 : N_{SR}$)
- m Index of the relay at receiving side of the communication link ($m = 1 : N_{RR}$)
- k Index of fault ($k = 1 : K$)
- g Index of synchronous generator ($g = 1 : G$)

Parameters

- OF Objective function
- T Total tripping times of main and back-up relays
- N_R Number of relays
- N_{PR} Number of primary relays
- N_{BR} Number of back-up relays
- N_{SR} Number of relays, sending a signal to another side of protection zones
- N_{RR} Number of relays, receiving a signal from another side of protection zones
- TDS_{R_n} Time dial setting of the relay at the n-th sending side of communication links
- PCS_{R_n} Pick-up current setting of the relay at the n-th sending side of communication links
- CTR Current transformer's ratio
- TDS^{min} Minimum permitted time dial settings
- TDS^{max} Maximum permitted time dial settings
- t^{NEF} Tripping time for a short circuit at the near-end of the protection zone

t^{FEF} Tripping time for a short circuit at the far-end of the protection zone
CTI Coordination time interval
t_{R_j,F_k} Tripping time of the j-th back-up relay for a short circuit at the k-th fault location
t_{R_i,F_k} Operating time of the i-th primary relay for a short circuit at the k-th fault location
CCT_{R_i,F_k} Critical clearing time of the i-th primary relay for a fault at the k-th fault location
$CCT_{R_i,F_k}^{SG_g}$ Critical clearing time of the i-th primary relay for a fault at the k-th fault location corresponding to the g-th distributed generation
S_{R_m,R_n} A communication signal, which is sent after tripping of the relay at one side of a protection zone to another side
$t_{F_k}^{R_m}$ Operating time of the m-th relay for a fault at the k-th fault location, which has sent a signal to another side of the protection zone.
$t_{F_k}^{R_n}$ Operating time of the n-th relay for a fault at the k-th fault location, which has received a signal from another side of the protection zone.
$\xi_{R_n}^{F_k}$ A Boolean variable, which it's one value represents that the current transmitting through the n-th relay-that received a signal from another side of the protection zone- is higher than the pick-up current
$I_{F_k}^{R_n}$ Short circuit current transmitting through the n-th relay that received a signal from another side of the protection zone
OF Objective function
TDS_r Time-dial setting of the r-th relay
PCS_r Pick-up current setting of the r-th relay
PCS_r^{min} Minimum allowed pick-up current setting of the r-th relay
PCS_r^{max} Maximum allowed pick-up current setting of the r-th relay

Abbreviations

A_{R_n} and B_{R_n} Coefficients of the standard tripping characteristic of the relay at the n-th sending side of communication links
BR Back-up relay
CCT Critical clearing times
CS_r An integer decision variable of the proposed optimization problem, representing the characteristic type of the r-th relay
CT Current transformer
CTI Coordination time interval
DG Distributed generation
DOCR Directional overcurrent relay
DPL DIgSILENT programming language
EI Extremely inverse
FEF Far-end fault
GA Genetic algorithm
LL Line-to-line
LLG Line-to-Line to the ground
LP Linear programming
MINLP Mixed-integer non-linear programming
NEF Near-end fault
NI Normally inverse
NLP Non-linear programming
OCR Overcurrent relay
OF Objective function (OF)
PCS Pick-up current setting
PR Primary relay
PSO Particle swarm optimization
SCC Short circuit current
SCF Short circuit fault
SG Synchronous generators
SLD Single line diagram
TCC Time-current curves
TDS Time dial setting
TLBO Teaching–learning-based optimization
VI Very inverse
WCA Water cycle algorithm

CONFLICT OF INTEREST

The authors declare that they have no known competing financial interests or personal relationships that could have appeared to influence the work reported in this paper.

FUNDING INFORMATION

The author(s) received no specific funding for this work.

DATA AVAILABILITY STATEMENT

Data available on request from the authors

ORCID

Hamed Hashemi-Dezaki https://orcid.org/0000-0003-2056-2388

REFERENCES

1. Gordon, S., McGarry, C., Bell, K.: The growth of distributed generation and associated challenges: A Great Britain case study. IET Renewable Power Gener., 1–14 (2022). https://doi.org/10.1049/rpg2.12416
2. Deakin, M., Morstyn, T., Apostolopoulou, D., McCulloch, M.D.: Voltage control loss factors for quantifying DG reactive power control impacts on losses and curtailment. IET Gener. Transm. Distrib. 16(10), 2049–2062 (2022). https://doi.org/10.1049/gtd2.12413
3. Kida, A.A., Labrador Rivas, A.E., Gallego, L.A.: An improved simulated annealing–linear programming hybrid algorithm applied to the optimal coordination of directional overcurrent relays. Electr. Power Syst. Res. 181, 106197 (2020). https://doi.org/10.1016/j.epsr.2020.106197
4. Ghaemi, S., Salehi, J., Moeini-Aghtaie, M.: Estimating abilities of distributed energy resources in providing flexible ramp products for active distribution networks. Sustainable Cities Soc. 65, 102593 (2021). https://doi.org/10.1016/j.scs.2020.102593
5. Jimada-Ojuolape, B., Teh, J.: Surveys on the reliability impacts of power system cyber–physical layers. Sustainable Cities Soc. 62, 102384 (2020). https://doi.org/10.1016/j.scs.2020.102384
6. Hasankhani, A., Mehdi Hakimi, S., Bisheh-Niasar, M., Shafie-khah, M., Asadolahi, H.: Blockchain technology in the future smart grids: A comprehensive review and frameworks. Int. J. Electr. Power Energy Syst. 129, 106811 (2021). https://doi.org/10.1016/j.ijepes.2021.106811
7. Hu, Y., Bu, S., Luo, J.: Application of energy flow analysis in investigating machine-side oscillations of full converter-based wind generation systems. IET Renewable Power Gener. 16(5), 900–911 (2022). https://doi.org/10.1049/rpg2.12387

8. Dorosti, P., Moazzami, M., Fani, B., Siano, P.: An adaptive protection coordination scheme for microgrids with optimum PV resources. J. Cleaner Prod. 340, 130723 (2022). https://doi.org/10.1016/j.jclepro.2022.130723
9. Khalid, H., Shobole, A.: Existing developments in adaptive smart grid protection: A review. Electr. Power Syst. Res. 191, 106901 (2021). https://doi.org/10.1016/j.epsr.2020.106901
10. Mohammadzadeh, N., Chabanloo, R.M., Maleki, M.G.: Optimal coordination of directional overcurrent relays considering two-level fault current due to the operation of remote side relay. Electr. Power Syst. Res. 175, 105921 (2019). https://doi.org/10.1016/j.epsr.2019.105921
11. Fayazi, H., Fani, B., Moazzami, M., Shahgholian, G.: An offline three-level protection coordination scheme for distribution systems considering transient stability of synchronous distributed generation. Int. J. Electr. Power Energy Syst. 131, 107069 (2021). https://doi.org/10.1016/j.ijepes.2021.107069
12. Hatata, A.Y., Ebeid, A.S., El-Saadawi, M.M.: Application of resistive super conductor fault current limiter for protection of grid-connected DGs. Alexandria Eng. J. 57(4), 4229–4241 (2018). https://doi.org/10.1016/j.aej.2018.11.009
13. Urdaneta, A.J., Restrepo, H., Marquez, S., Sanchez, J.: Coordination of directional overcurrent relay timing using linear programming. IEEE Trans. Power Delivery 11(1), 122–129 (1996). https://doi.org/10.1109/61.484008
14. Poursaeed, A.H., Namdari, F.: Real-time voltage stability monitoring using weighted least square support vector machine considering overcurrent protection. Int. J. Electr. Power Energy Syst. 136, 107690 (2022). https://doi.org/10.1016/j.ijepes.2021.107690
15. Alam, M.N., Das, B., Pant, V.: An interior point method based protection coordination scheme for directional overcurrent relays in meshed networks. Int. J. Electr. Power Energy Syst. 81, 153–164 (2016). https://doi.org/10.1016/j.ijepes.2016.02.012
16. Ghotbi-Maleki, M., Mohammadi Chabanloo, R., Askarian Abyaneh, H., Zamani, M.: Considering transient short-circuit currents of wind farms in overcurrent relays coordination using binary linear programming. Int. J. Electr. Power Energy Syst. 131, 107086 (2021). https://doi.org/10.1016/j.ijepes.2021.107086
17. Noghabi, A.S., Sadeh, J., Mashhadi, H.R.: Considering different network topologies in optimal overcurrent relay coordination using a hybrid GA. IEEE Trans. Power Delivery 24(4), 1857–1863 (2009). https://doi.org/10.1109/TPWRD.2009.2029057
18. Razavi, F., Abyaneh, H.A., Al-Dabbagh, M., Mohammadi, R., Torkaman, H.: A new comprehensive genetic algorithm method for optimal overcurrent relays coordination. Electr. Power Syst. Res. 78(4), 713–720 (2008). https://doi.org/10.1016/j.epsr.2007.05.013
19. Samadi, A., Mohammadi Chabanloo, R.: Adaptive coordination of overcurrent relays in active distribution networks based on independent change of relays' setting groups. Int. J. Electr. Power Energy Syst. 120, 106026 (2020). https://doi.org/10.1016/j.ijepes.2020.106026
20. Korashy, A., Kamel, S., Youssef, A.-R., Jurado, F.: Modified water cycle algorithm for optimal direction overcurrent relays coordination. Appl. Soft Comput. 74, 10–25 (2019). https://doi.org/10.1016/j.asoc.2018.10.020
21. Sarwagya, K., Nayak, P.K., Ranjan, S.: Optimal coordination of directional overcurrent relays in complex distribution networks using sine cosine algorithm. Electr. Power Syst. Res. 187, 106435 (2020). https://doi.org/10.1016/j.epsr.2020.106435
22. Saldarriaga-Zuluaga, S.D., López-Lezama, J.M., Muñoz-Galeano, N.: Optimal coordination of over-current relays in microgrids considering multiple characteristic curves. Alexandria Eng. J. 60(2), 2093–2113 (2021). https://doi.org/10.1016/j.aej.2020.12.012
23. Darabi, A., Bagheri, M., Gharehpetian, G.B.: Highly sensitive microgrid protection using overcurrent relays with a novel relay characteristic. IET Renewable Power Gener. 14(7), 1201–1209 (2020)
24. Narimani, A., Hashemi-Dezaki, H.: Optimal stability-oriented protection coordination of smart grid's directional overcurrent relays based on optimized tripping characteristics in double-inverse model using high-set relay. Int. J. Electr. Power Energy Syst. 133, 107249 (2021). https://doi.org/10.1016/j.ijepes.2021.107249
25. Yazdaninejadi, A., Nazarpour, D., Golshannavaz, S.: Sustainable electrification in critical infrastructure: Variable characteristics for overcurrent protection considering DG stability. Sustainable Cities Soc. 54, 102022 (2020). https://doi.org/10.1016/j.scs.2020.102022
26. Yigit, K., Acarkan, B.: A new electrical energy management approach for ships using mixed energy sources to ensure sustainable port cities. Sustainable Cities Soc. 40, 126–135 (2018). https://doi.org/10.1016/j.scs.2018.04.004
27. Ministry of Energy of Iran, Iran's electricity industry for strategic management (2019). https://isn.moe.gov.ir/
28. Urdaneta, A.J., Pérez, L.G., Gómez, J.F., Feijoo, B., González, M.: Presolve analysis and interior point solutions of the linear programming coordination problem of directional overcurrent relays. Int. J. Electr. Power Energy Syst. 23(8), 819–825 (2001). https://doi.org/10.1016/S0142-0615(00)00097-1
29. Elmitwally, A., Gouda, E., Eladawy, S.: Optimal allocation of fault current limiters for sustaining overcurrent relays coordination in a power system with distributed generation. Alexandria Eng. J. 54(4), 1077–1089 (2015). https://doi.org/10.1016/j.aej.2015.06.009
30. Elmitwally, A., Gouda, E., Eladawy, S.: Restoring recloser-fuse coordination by optimal fault current limiters planning in DG-integrated distribution systems. Int. J. Electr. Power Energy Syst. 77, 9–18 (2016). https://doi.org/10.1016/j.ijepes.2015.11.021
31. Bouchekara, H.R.E.H., Zellagui, M., Abido, M.A.: Optimal coordination of directional overcurrent relays using a modified electromagnetic field optimization algorithm. Appl. Soft Comput. 54, 267–283 (2017). https://doi.org/10.1016/j.asoc.2017.01.037
32. Sharaf, H.M., Zeineldin, H.H., El-Saadany, E.: Protection coordination for microgrids with grid-connected and islanded capabilities using communication assisted dual setting directional overcurrent relays. IEEE Trans. Smart Grid 9(1), 143–151 (2018). https://doi.org/10.1109/TSG.2016.2546961
33. Orazgaliyev, D., Tleubayev, A., Zholdaskhan, B., Nunna, H.S.V.S.K., Dadlani, A., Doolla, S.: Adaptive coordination mechanism of overcurrent relays using evolutionary optimization algorithms for distribution systems with DGs. In: *2019 International Conference on Smart Energy Systems and Technologies (SEST)*, pp. 1–6. Porto, Portugal (2019). https://doi.org/10.1109/SEST.2019.8849052
34. Aghdam, T.S., Karegar, H.K., Zeineldin, H.H.: Optimal coordination of double-inverse overcurrent relays for stable operation of DGs. IEEE Trans. Ind. Inf. 15(1), 183–192 (2019). https://doi.org/10.1109/TII.2018.2808264
35. Hemmati, R., Mehrjerdi, H.: Non-standard characteristic of overcurrent relay for minimum operating time and maximum protection level. Simul. Modell. Pract. Theory 97, 101953 (2019). https://doi.org/10.1016/j.simpat.2019.101953
36. Alam, M.N.: Adaptive protection coordination scheme using numerical directional overcurrent relays. IEEE Trans. Ind. Inf. 15(1), 64–73 (2019). https://doi.org/10.1109/TII.2018.2834474
37. El-Naily, N., Saad, S.M., Mohamed, F.A.: Novel approach for optimum coordination of overcurrent relays to enhance microgrid earth fault protection scheme. Sustainable Cities Soc. 54, 102006 (2020). https://doi.org/10.1016/j.scs.2019.102006
38. Alam, M.N., Das, B., Pant, V.: Protection coordination scheme for directional overcurrent relays considering change in network topology and OLTC tap position. Electr. Power Syst. Res. 185, 106395 (2020). https://doi.org/10.1016/j.epsr.2020.106395
39. Elmitwally, A., Kandil, M.S., Gouda, E., Amer, A.: Mitigation of DGs impact on variable-topology meshed network protection system by optimal fault current limiters considering overcurrent relay coordination. Electr. Power Syst. Res. 186, 106417 (2020). https://doi.org/10.1016/j.epsr.2020.106417
40. Entekhabi-Nooshabadi, A.M., Hashemi-Dezaki, H., Taher, S.A.: Optimal microgrid's protection coordination considering N-1 contingency and optimum relay characteristics. Appl. Soft Comput. 98, 106741 (2021). https://doi.org/10.1016/j.asoc.2020.106741

41. Saldarriaga-Zuluaga, S.D., López-Lezama, J.M., Muñoz-Galeano, N.: Adaptive protection coordination scheme in microgrids using directional over-current relays with non-standard characteristics. Heliyon 7(4), e06665 (2021). https://doi.org/10.1016/j.heliyon.2021.e06665
42. Khoshbakht, E., Namdari, F., Doostizadeh, M.: Effects of protection settings on optimal performance of reconfigurable smart distribution systems. IET Renewable Power Gener. 15(8), 1678–1692 (2021)
43. Sadeghi, M.H., Dastfan, A., Damchi, Y.: Optimal coordination of directional overcurrent relays in distribution systems with DGs and FCLs considering voltage sag energy index. Electr. Power Syst. Res. 191, 106884 (2021). https://doi.org/10.1016/j.epsr.2020.106884
44. Hatata, A.Y., Ebeid, A.S., El-Saadawi, M.M.: Optimal restoration of directional overcurrent protection coordination for meshed distribution system integrated with DGs based on FCLs and adaptive relays. Electr. Power Syst. Res. 205, 107738 (2022). https://doi.org/10.1016/j.epsr.2021.107738
45. Razzaghi, R., Davarpanah, M., Sanaye-Pasand, M.: A novel protective scheme to protect small-scale synchronous generators against transient instability. IEEE Trans. Ind. Electron. 60(4), 1659–1667 (2013). https://doi.org/10.1109/TIE.2012.2186773
46. Guo, Z., et al.: Control and capacity planning for energy storage systems to enhance the stability of renewable generation under weak grids. IET Renewable Power Gener. 16(4), 761–780 (2022). https://doi.org/10.1049/rpg2.12424
47. Chandra, A., Pradhan, A.K.: Model-free angle stability assessment using wide area measurements. Int. J. Electr. Power Energy Syst. 120, 105972 (2020). https://doi.org/10.1016/j.ijepes.2020.105972
48. Darabi, A., Bagheri, M., Gharehpetian, G.B.: Highly reliable overcurrent protection scheme for highly meshed power systems. Int. J. Electr. Power Energy Syst. 119, 105874 (2020). https://doi.org/10.1016/j.ijepes.2020.105874
49. Iqbal, J., et al.: A generic internet of things architecture for controlling electrical energy consumption in smart homes. Sustainable Cities Soc. 43, 443–450 (2018). https://doi.org/10.1016/j.scs.2018.09.020.
50. Aghdam, T.S., Karegar, H.K., Zeineldin, H.H.: Transient stability constrained protection coordination for distribution systems with DG. IEEE Trans. Smart Grid 9(6), 5733–5741 (2018). https://doi.org/10.1109/TSG.2017.2695378
51. Ghotbi Maleki, M., Mohammadi Chabanloo, R., Taheri, M.R.: Mixed-integer linear programming method for coordination of overcurrent and distance relays incorporating overcurrent relays characteristic selection. Int. J. Electr. Power Energy Syst. 110, 246–257 (2019). https://doi.org/10.1016/j.ijepes.2019.03.007
52. Zare, J., Pirooz Azad, S.: A new relaying scheme for protection of transmission lines connected to DFIG-based wind farms. IET Renewable Power Gener. 15(13), 2971–2982 (2021). https://doi.org/10.1049/rpg2.12232
53. Alam, M.N., Chakrabarti, S., Pradhan, A.K.: Protection of networked microgrids using relays with multiple setting groups. IEEE Trans. Ind. Inf. 18(6), 3713–3723 (2021). https://doi.org/10.1109/TII.2021.3120151
54. Dindar, A., Ardehali, M.M., Vakilian, M.: Integration of wind turbines in distribution systems and development of an adaptive overcurrent relay coordination scheme with considerations for wind speed forecast uncertainty. IET Renewable Power Gener. 14(15), 2983–2992 (2020). https://doi.org/10.1049/iet-rpg.2020.0786
55. Reda, A., Abdelgawad, A.F., Ibrahim, M.: Effect of non standard characteristics of overcurrent relay on protection coordination and maximizing overcurrent protection level in distribution network. Alexandria Eng. J. 61(9), 6851–6867 (2022). https://doi.org/10.1016/j.aej.2021.12.034
56. Kalage, A.A., Ghawghawe, N.D.: Optimum coordination of directional overcurrent relays using modified adaptive teaching learning based optimization algorithm. Intell. Ind. Syst. 2(1), 55–71 (2016). https://doi.org/10.1007/s40903-016-0038-9
57. Karimi, H., Fani, B., Shahgholian, G.: Multi agent-based strategy protecting the loop-based micro-grid via intelligent electronic device-assisted relays. IET Renewable Power Gener. 14(19), 4132–4141 (2020). https://doi.org/10.1049/iet-rpg.2019.1233
58. Abbaspour, E., Fani, B., Karami-Horestani, A.: Adaptive scheme protecting renewable-dominated micro-grids against usual topology-change events. IET Renewable Power Gener. 15(12), 2686–2698 (2021). https://doi.org/10.1049/rpg2.12193
59. IEEE guide for the application of current transformers used for protective relaying purposes. In: IEEE Std C37.110-2007 (Revision of Std C37.110-1996), pp. 1–90. IEEE, Piscataway, NJ (2008). https://doi.org/10.1109/IEEESTD.2008.4483716

How to cite this article: Aghaei, H., Hashemi-Dezaki, H.: Optimal communication-aided protection of meshed smart grids considering stability constraints of distributed generations incorporating optimal selection of relay characteristics. IET Renew. Power Gener. 16, 2313–2337 (2022). https://doi.org/10.1049/rpg2.12525